

c.1

A CONVERTER MODEL  
FOR THE DIGITAL SIMULATION OF TRANSIENTS  
IN AC/DC TRANSMISSION SYSTEMS



by

BÜT-CHUNG CHIU

B.E.E., University of Minnesota, 1974

A THESIS SUBMITTED IN PARTIAL FULFILLMENT OF  
THE REQUIREMENTS FOR THE DEGREE OF  
MASTER OF APPLIED SCIENCE

in

THE FACULTY OF GRADUATE STUDIES  
Department of Electrical Engineering

We accept this thesis as conforming  
to the required standard

THE UNIVERSITY OF BRITISH COLUMBIA

May, 1980



But-chung Chiu, 1980

In presenting this thesis in partial fulfilment of the requirements for an advanced degree at the University of British Columbia, I agree that the Library shall make it freely available for reference and study. I further agree that permission for extensive copying of this thesis for scholarly purposes may be granted by the Head of my Department or by his representatives. It is understood that copying or publication of this thesis for financial gain shall not be allowed without my written permission.

Department of ELECTRICAL ENGINEERING

The University of British Columbia  
2075 Wesbrook Place  
Vancouver, Canada  
V6T 1W5

Date MAY 30, 1980

## ABSTRACT

The successful application of HVDC transmission links requires correct predictions of the performance of the dc link and the ac system to which it is interconnected. Whatever the system configuration, the steady-state, dynamic and transient behaviour of the associated dc and ac systems are mostly interdependent. To simulate these phenomena with digital computers, converter stations must be modelled in more detail than as simple dc sources.

This thesis discusses the development and implementation of a converter model which enables the converter bridge circuits to be represented in detail and the valve ignition to be controlled in the constant current mode. The model has been added to the U.B.C. Electromagnetic Transients Program to permit simulations of the complete ac/dc system. It is used to analyze the harmonics during steady-state operation, and to compare the results with those obtained from conventional (approximate) formulae. In a transient case, the new model gives closer agreement with field measurements than the simplified model used before.

# T A B L E    O F    C O N T E N T S

---

	<u>Page</u>
ABSTRACT . . . . .	ii
TABLE OF CONTENTS . . . . .	iii
LIST OF TABLES . . . . .	v
LIST OF ILLUSTRATIONS . . . . .	vi
ACKNOWLEDGEMENTS . . . . .	vii
1. INTRODUCTION . . . . .	1
2. MODELLING AN HVDC TRANSMISSION SYSTEM . . . . .	4
2.1 Network Representation . . . . .	4
2.2 The Converter . . . . .	5
2.3 Converter Control Characteristics . . . . .	8
3. IMPLEMENTATION OF THE CONVERTER MODEL . . . . .	14
3.1 Subroutine VALCON . . . . .	14
3.2 Limiter Representation . . . . .	18
3.3 Initialization . . . . .	23
4. HARMONIC ANALYSIS . . . . .	30
4.1 Analyzing Method . . . . .	30
4.2 Harmonic Contents . . . . .	32
4.3 Abnormal Harmonics . . . . .	36
5. TRANSIENTS SIMULATION . . . . .	39
5.1 Point to Point Operation . . . . .	39
5.2 Three Terminal Operation . . . . .	41

	<u>Page</u>
6. CONCLUSIONS . . . . .	46
REFERENCE . . . . .	48
APPENDIX 1      Subroutine VALCON Programme Listings . . . . .	50
APPENDIX 2      Modifications in the Transients Program . . . . .	54
APPENDIX 3      Fourier Analysis Programme Listings . . . . .	59
APPENDIX 4      Line Parameters and Converter Station Parameters of the Pacific HVDC Intertie . . . . .	61
APPENDIX 5      Input Listings of the Point to Point Operation Simulation . . . . .	65
APPENDIX 6      Sample Data Deck of the Three-Terminal Operation Simulation . . . . .	71

# LIST OF TABLES

<u>Table</u>		<u>Page</u>
4.1	Comparison of current harmonics obtained from theoretical calculations and from Fourier analysis of simulated curves.....	34
4.2	Comparison of dc voltage harmonics under balanced operation and imbalance in magnitude and phase in one phase of the ac bus.....	37
5.1	Steady-state system parameters before fault.....	42
A2.1	Changes in the Transients Program for data transferred to subroutine VALCON.....	55
A4.1	Transmission line data of the Pacific HVDC Intertie.....	63

# L I S T   O F   I L L U S T R A T I O N S

<u>Figure</u>	<u>Page</u>
2.1 Basic HVDC link.....	6
2.2 Basic hardware of a converter bridge.....	6
2.3 Direct voltage (heavy lines) of bridge converter with variation of ignition delay angle $\alpha$ .....	7
2.4 Constant current controller.....	8
2.5 Control characteristic of converter .....	10
2.6 Two-converter control characteristic.....	10
2.7 Relationship between dc voltage $V_d$ and regulator output $e_{\alpha}$ .....	12
3.1 Flow chart of the simulation.....	17
3.2 Control amplifier circuit.....	18
3.3 Three operating regions of the control amplifier.....	20
3.4 Response of the current regulator when subject to a saw-toothed disturbance.....	22
3.5 System set up for initialization.....	24
3.6 Long run to verify steady state solution.....	26
3.7 Simulation with dc starts at (a) a point of commutation; (b) middle of non-commutation interval.....	27
3.8 Simulation results with electrode line starts at zero initial condition.....	28
4.1 Simulated ac characteristic harmonic current for 6-pulse operation.....	35
4.2 Harmonic voltage on the dc side of the rectifier terminal.....	38
5.1 Comparison between simplified and detailed converter station models for a fault on the dc line.....	40
5.2 System configuration for dc circuit breaker test .....	42
5.3 Current through dc breaker following a close-in fault.....	43
5.4 Current through dc breaker following a remote fault.....	44
A4.1 Main circuit of Pacific HVDC Intertie.....	62
A4.2 Converter bridge at Celilo.....	63
A4.3 Filter arrangement at Celilo.....	64

## ACKNOWLEDGEMENT

I would like to express my sincere thanks to my supervisor, Dr. H.W. Dommel, for his inspiring guidance, unflagging patience and continued encouragement during my period of graduate study. I am also deeply grateful to Dr. M.S. Davies for his interest and timely advice during the research work.

The financial assistance and the invaluable discussions of the project with engineers of the System Engineering Division of B.C. Hydro and Power Authority are gratefully acknowledged.

Special thanks are due to Mrs. K. Brindamour of the Department of Electrical Engineering for her proficient typing of this thesis.

I am greatly indebted to my mother and the members of my family for their patience and encouragement throughout my university studies.



## 1 . I N T R O D U C T I O N

Power system networks are subjected to different forms of disturbances, such as switching operations, faults, lightning surges, and other intended or unintended manual interventions. The overvoltages and currents caused by these sudden changes in circuit conditions may produce excessive stresses on the system components which must be prevented, or at least limited, to avoid potential damages. More insulation is one way of preventing excessive stresses, but there are strong economic reasons for keeping the system insulation at its lowest possible level. This can be achieved only if the transient phenomena are fully analyzed.

Extended from the idea of a-c calculating boards, the transient network analyzer (TNA) was developed for transient studies<sup>1</sup>. It has been widely used by the utility industry for over forty years. The system being studied is represented by actual components of reduced size and modified electrical characteristics. It is particularly useful in modelling the frequency dependent characteristics of the line constants and in those cases where the work is of exploratory nature. However, the transmission lines are approximated by cascaded  $\pi$ -circuits, which impose an accuracy problem as far as high-frequency components of voltage and current are concerned. Another drawback of this method is the limited access to the sophisticated equipment.

The introduction of computers has extended the scope of the mathematical modelling in solving engineering problems. Digital programming today offers a relatively easy and flexible alternative to the physical models in power system analysis. In the late 1960's, the Bonneville Power Adminis-

tration (BPA) initiated the development of the Electromagnetic Transients Program (EMTP)<sup>2</sup> which simulates the behaviour of the electrical system by using mathematical representations of the characteristics of the components and by solving a set of differential and algebraic matrix equations. The generalized access to computers, the flexibility of the EMTP for running cases, and the relative ease with which program changes can be made are the main reasons of its widespread acceptance. Of course, there are many areas such as frequency-dependent characteristics, nonlinearity of surge diverters, magnetic saturation of transformers, etc., which need further improvements. A combination of physical models and digital simulation can be extremely powerful and the two approaches should be seen as being complementary rather than competitive<sup>5</sup>.

With the advent of the economic feasibility and technical applicability of HVDC transmission, there is a need for an extension of the existing facilities to carry out DC transient studies. The DC simulator uses the same control circuitry and a scaled reproduction of the commutation valves of the actual system<sup>3,4</sup>. When interconnected with the traditional a-c TNA, it becomes particularly valuable in development and evaluation of the control schemes. During the same period of time, considerable amount of work has been done in the field of digital simulation of HVDC systems. Additional features have also been implemented in the BPA EMTP for this purpose: a simplified model which represents the converter station as a current controlled dc voltage source<sup>6</sup> and a control system simulation package "TACS" (Transient Analysis of Control Systems)<sup>7</sup> which can accept any arbitrary interconnection of a set of control system building blocks. Good results obtained by using these two models are shown in reference papers<sup>8,9</sup>.

The UBC Transients Program (a simpler version of the BPA EMTP)

contains only the simplified model which is inadequate for representing a combined ac/dc system. "TACS" is very flexible and can be used for a wide range of applications. However, it is relatively large and usually requires a fairly long computation time. The major research effort of this thesis has been directed towards the development of a new converter model which can be interfaced with the UBC Transients Program for HVDC simulations. The model is complex enough to analyze transients in ac/dc systems realistically enough, but it is less flexible than "TACS" inasmuch as only one particular type of converter control can be handled.

As the thesis proceeds, the implementation and testing of the model are described. New approaches in representing the limiters and the initialization process are investigated. Then the program is applied to harmonic analysis and transient studies where the comparisons with results obtained by other methods and field measurements are also included. Finally, a summary of important results and conclusions is given.

## 2. MODELLING AN HVDC TRANSMISSION SYSTEM

To provide accurate predictions on the performance of an HVDC system under different operating conditions, the simulation method should be capable of representing the dc link, the associated ac systems, the converters and the controls as well. This chapter describes the main components of an HVDC system and their behaviour which the model must reflect correctly.

### 2.1 Network Representation

The basic components of a dc link between two ac systems are shown in Fig. 2.1. The basis for the simulation is the UBC Electromagnetic Transients Program. For convenience, it will be referred to as the "Transients Program". It is a general purpose program designed to calculate the instantaneous voltages and currents under any type of disturbance. The solution methods and its applicabilities have been well described<sup>2,10,11</sup>. The existing models in the Transients Program are adequate to simulate most circuit elements in both the ac and dc side networks. The dc transmission configuration can be monopolar, bipolar, ground return or metallic return. The transmission lines are represented either as multiphase  $\pi$  circuits or distributed constants. The ac and dc filters which comprise branches tuned to different harmonic orders of the supply frequency are represented as lumped R, L, C elements according to their connections in the system. Although zigzag winding, fork connection, polygon connection etc., are used in some commercial installations, the converter transformer can only be modelled with wye and delta connections as of now. The amount of detail in the representation of the ac systems depends on the nature of the study.

They may be represented with detailed generator and line models, or just as ac voltage sources behind Thevenin equivalent impedances.

## 2.2 The Converter

It is the predominant device in an HVDC system which transforms an ac voltage into a dc voltage and vice versa, controls the exchange of power between the two systems, and limits the disturbances caused by faults occurring on either side of the converting unit. The most commonly used circuit in HVDC transmission is the six-pulse bridge. Fig. 2.2 shows the basic hardware requirement. The valves can be mercury-arc valves or silicon controlled rectifiers. The valve dampers are used to avoid sudden jumps in the inverse voltage across the valves when they turn off (dv/dt protection), while the anode dampers limit the rate of rise of current during valve ignition (di/dt protection).

The performance of a converter bridge is controlled by changing the firing angle,  $\alpha$ , of the valves. Fig. 2.3 shows how the dc voltage is effected by variations in  $\alpha$ . As  $\alpha$  exceeds  $90^\circ$ , the bridge changes from rectification operation to inversion operation. To minimize the generation of harmonics, the bridge units are usually paired with wye/wye and delta/wye transformers, with a phase shift of  $30^\circ$  between them, to form a 12-pulse unit. These 12-pulse units are themselves connected in series to produce the required transmission voltage level.

To simulate the operation of the valves, the existing model of a diode switch, which conducts whenever the anode voltage is higher than the cathode voltage and interrupts at current zero, is modified so that the ignition is controlled by an external firing signal. The characteristics of

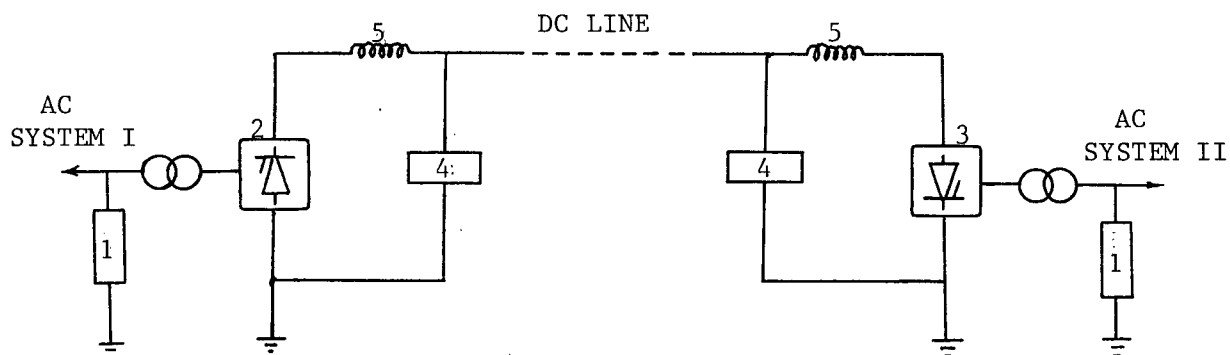


Fig. 2.1 Basic HVDC Link: 1 - AC filters; 2 - Rectifier station; 3 - Inverter station; 4 - DC filters; 5 - DC reactors.

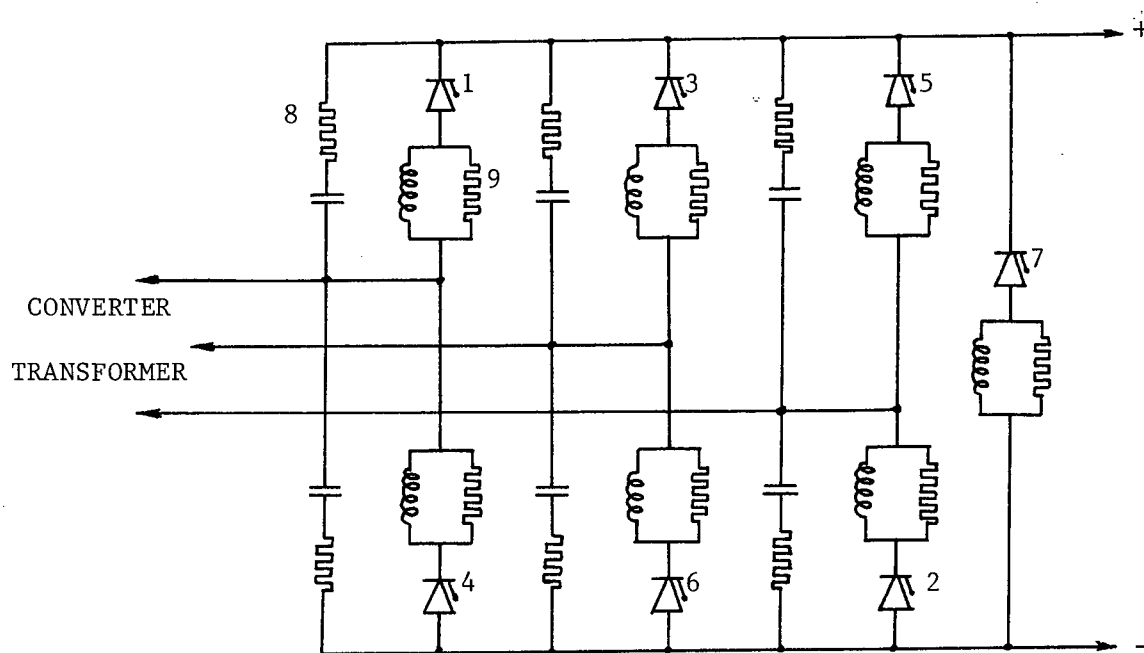


Fig. 2.2 Basic Hardware of a converter bridge: 1 to 6 - Main valves; 7 - Bypass valve; 8 - Valve damper; 9 - Anode damper.

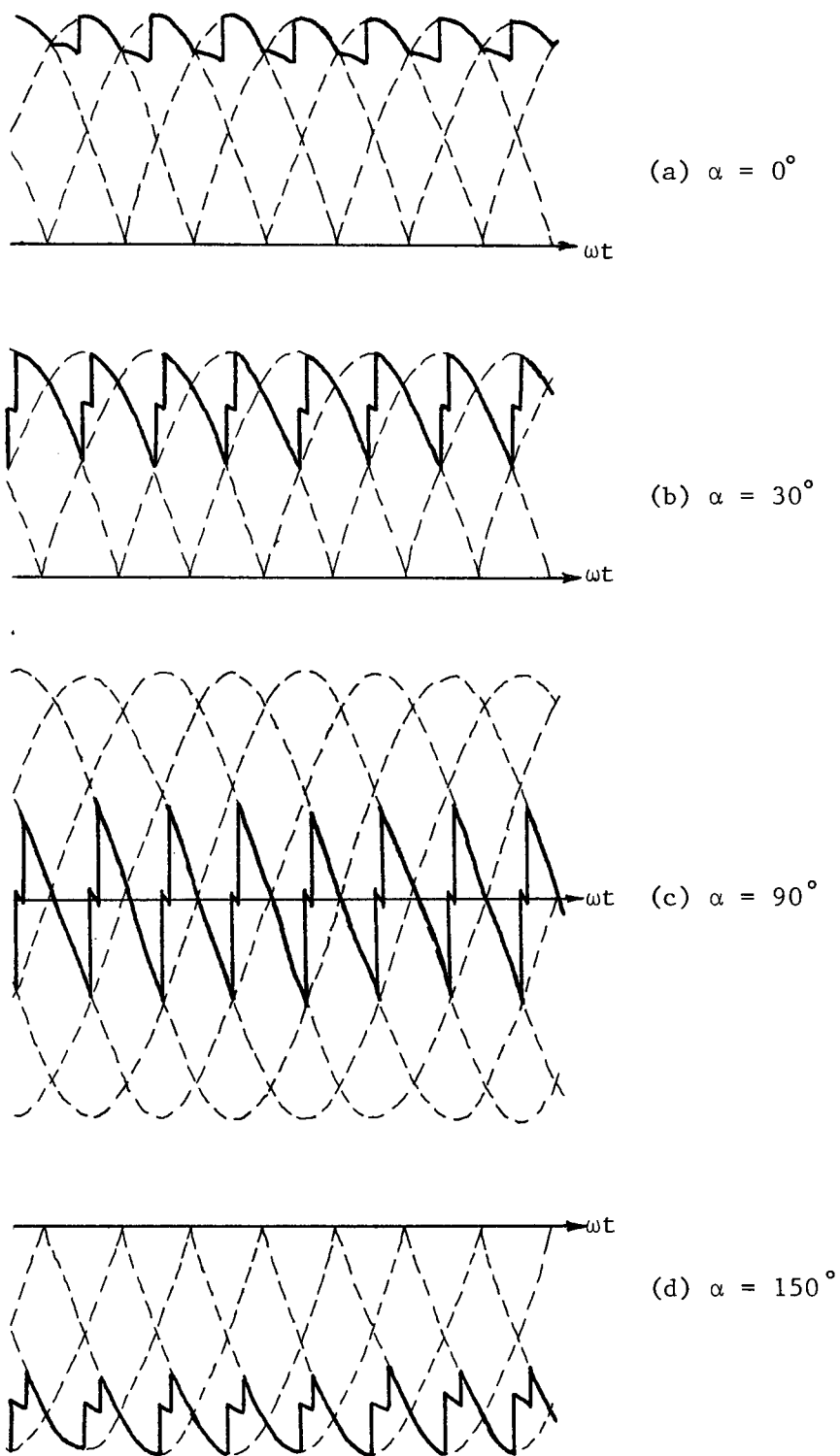


Fig. 2.3 Direct voltage (heavy lines) of bridge converter with variation of ignition delay angle  $\alpha$  :  
 (a), (b) - Rectification; (c) - Zero voltage;  
 (d) - Inversion.

the control systems and the generation of the firing pulses will be described in the next section.

### 2.3 Converter Control Characteristics

The control loop of rectification is generally a constant current loop<sup>12</sup>. The schematic diagram of the basic components of such a controller is shown in Fig. 2.4. Recent installations contain additional and more sophisticated schemes, such as constant power order, dc power modulation or frequency modulation for ac system damping, etc. These latter applications are extensions of the former and the variables under control are ultimately converted into changes of current order. For electromagnetic transients analysis, the constant current controller plays the most significant part. Therefore, to simplify the modelling, only this control scheme is implemented in the program.

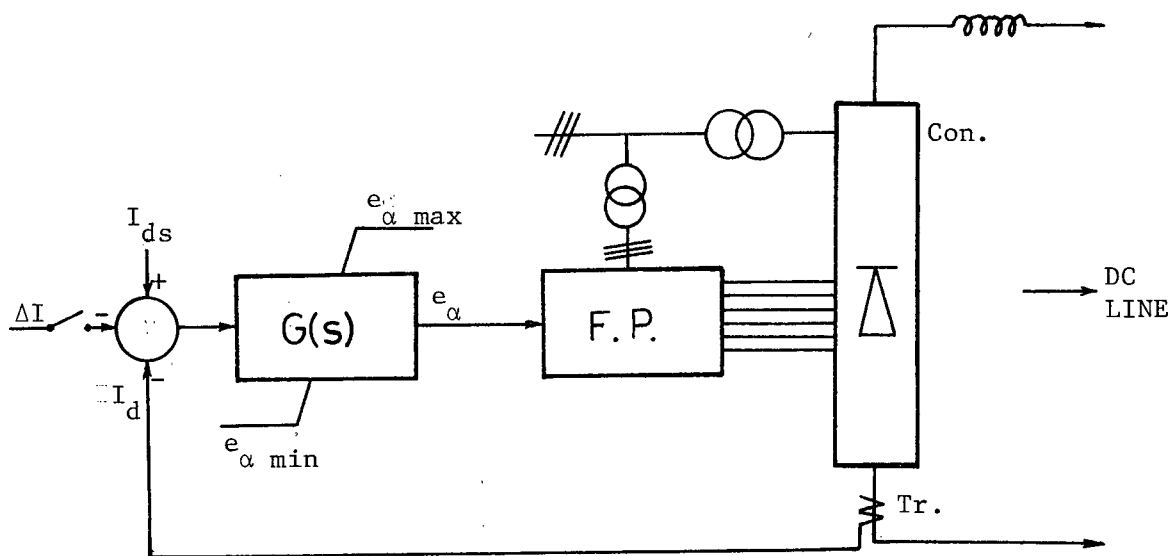


Fig. 2.4 Constant Current Controller :  $I_{ds}$  current command;  $I_d$  line current ;  $\Delta I$  current margin;  $G(s)$  regulator transfer function ;  $e_{\alpha}$  regulator output;  $e_{\alpha \max}$ ,  $e_{\alpha \min}$  limits of regulator; Con. converter; F.P. firing pulse generation; Tr. transducer.



The control characteristics may be divided into three sections<sup>13,14</sup> (Fig. 2.5): (1) Constant minimum ignition angle (C.I.A.) control is used to keep the rectifier operating with its minimum permissible firing delay  $\alpha_0$ . The theoretical minimum  $\alpha_0$  equals zero, but in practice it is kept to between  $10^\circ$  to  $20^\circ$  in order to maintain an adequate margin for rapid increases in rectifier voltage. The slope of the curve in this section depends upon the value of commutating reactance; the output voltage of the converter is given by,

$$V_d = V_{do} \cos \alpha_0 - \frac{3}{\pi} X_c I_d \quad (2.1)$$

where  $V_d$  = average converter voltage,

$V_{do}$  = converter ideal no-load direct voltage,

$\alpha_0$  = minimum delay angle,

$X_c$  = commutating reactance per phase,

$I_d$  = dc line current.

(2) Constant Current (C.C.) Control is used to provide both the rectifier and inverter with the control ability to regulate the line current when it does not agree with a set reference  $I_{ds}$ . The slope of the curve depends mainly on the output of the current regulator, and the output voltage is given by,

$$V_d = V_{do} \cos \alpha - \frac{3}{\pi} X_c I_d \quad (2.2)$$

where  $\alpha$  = angle of delay of firing.

(3) Constant Extinction Angle (C.E.A.) Control is used to keep the inverter operating at its minimum extinction advance angle. The angle must be kept small to provide high power factor but large enough to maintain a safe margin to prevent commutation failures. The slope of the curve again depends on the value of the commutating reactance, and the output voltage of the converter is given by

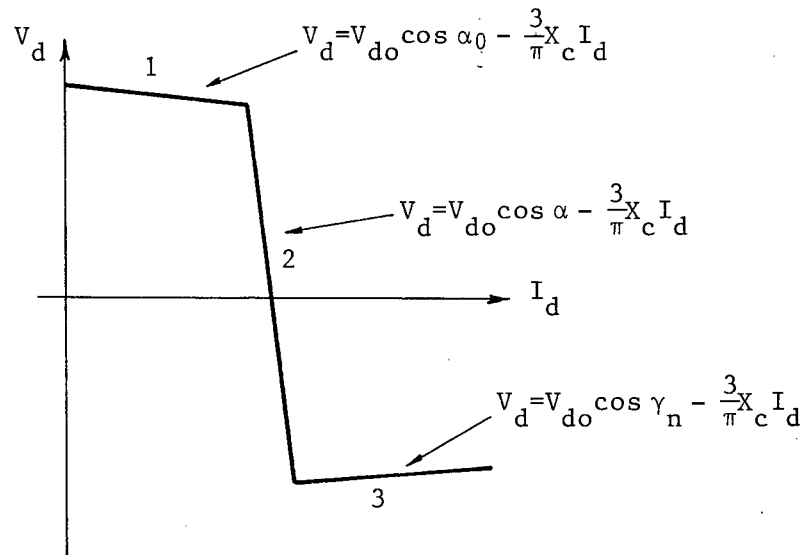


Fig. 2.5 Control Characteristic of Converter: 1 - C.I.A. control; 2 - C.C. control; 3 - C.E.A. control.

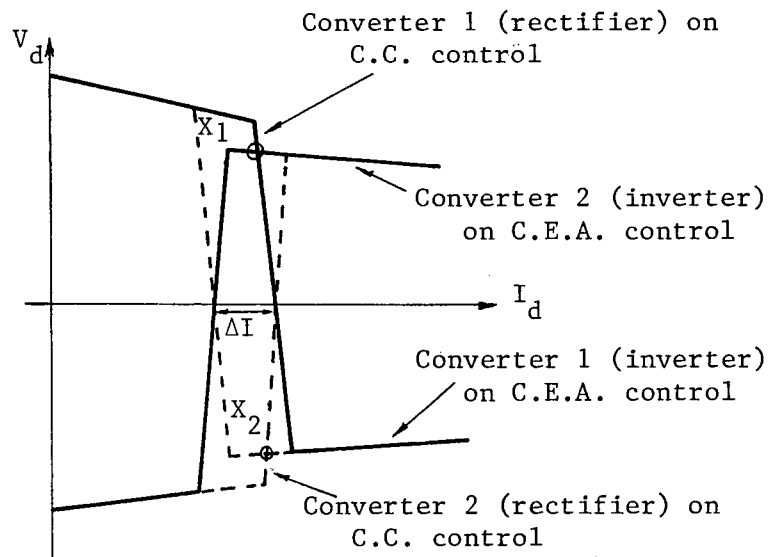


Fig. 2.6 Two-converter Control Characteristic.

$$V_d = V_{do} \cos \gamma_n - \frac{3}{\pi} X_c I_d \quad (2.3)$$

where  $\gamma_n$  = minimum extinction advance angle.

For a two-converter system, the operating point is at the intersection of the two control characteristics. In Fig. 2.6, the intersection  $X_1$  between the solid lines is the operating point where converter 1 is at constant current mode and converter 2 at constant extinction angle mode. Power is transmitted from converter 1 to converter 2. If a reversal of power transmission is necessary, the characteristics are changed to those shown by the broken lines and  $X_2$  will become the operating point. The difference between the current settings  $I_{ds1}$  and  $I_{ds2}$  of the two converters is called the current margin,  $\Delta I$ . This margin, typically 15% of the rated current, has to be large enough to avoid the two converters from operating at the steep constant-current lines simultaneously. Such operation is undesirable and may also be very unstable.

The operating mode of a converter is determined by the control amplifier output voltage  $e_\alpha$ . As seen from Fig. 2.4,

$$e_\alpha(s) = (I_{ds} - I_d - \Delta I) G(s) \quad (2.4)$$

The parameters of the transfer function  $G(s)$  can be obtained from the station operating manuals<sup>15</sup>. The transfer function of the control scheme studied in this thesis is a second order one of the form

$$G(s) = \frac{K(1+sT_2)}{(1+sT_1)(1+sT_3)} \quad (2.5)$$

where  $K$  is the static gain

and  $T_1$ ,  $T_2$ ,  $T_3$  are time constants.

The other settings depend on the operating conditions of the system. Different amplifier output voltages lead the converter to different operating regions:

- a) if  $e_{\alpha \max} > e_{\alpha} > e_{\alpha \min}$ , the converter operates in region '2'  
(see Fig. 2.5), i.e. on C.C. Control.
- b) if  $e_{\alpha} < e_{\alpha \min}$ , the converter operates in region '3',  
i.e. C.E.A. Control.
- c) if  $e_{\alpha} > e_{\alpha \max}$ , the converter operates in region '1',  
i.e. C.I.A. Control.

As shown in Fig. 2.7, the direct voltage  $V_d$  is a function of  $e_{\alpha}$  and can be described as<sup>6</sup>:

$$V_d = k_1 + k_2 e_{\alpha} \quad (2.6)$$

where  $k_1$  = intercept,

$k_2$  = slope of the converter constant current control characteristic.

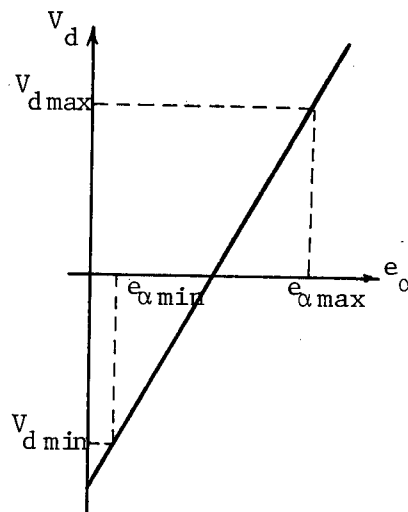


Fig. 2.7 Relationship between D.C. voltage  $V_d$  and regulator output  $e_{\alpha}$

Knowing the value of  $V_d$  and the operating region of the converter, the delay angle  $\alpha$  can be calculated from equations 2.1, 2.2 or 2.3. Then the pulse generator determines the firing instant for each valve. There are two basic approaches in the design of pulse generators:

- 1) Individual phase control: Six independent delay circuits time the firing pulse of each valve. The delay is calculated from the earliest instant at which firing is possible, that is, the instant at which the commutating voltage becomes positive. This type of control has the advantage that it can achieve the highest possible direct voltage with the asymmetry prevailing at the time. However, it has a drawback inasmuch as abnormal harmonics, especially of the third order, appear in the currents.
- 2) Equidistant firing control (or 'equal space' control)<sup>16</sup>: There is always one reference phase at which the firing angle is determined according to the control amplifier output. Starting with this angle, each firing pulse is timed at  $60^\circ$  electrical after the preceding pulse, that is, the valves are ignited at equal time intervals. As a result, abnormal harmonics are suppressed but the response in the event of a fault is slower.

### 3. IMPLEMENTATION OF THE CONVERTER MODEL

This chapter describes the solution method and the computer implementation of the converter model. Also included is a discussion of the two major problems encountered during the implementation.

#### 3.1 Subroutine VALCON

To simulate the converter control of the HVDC system, a subroutine VALCON ("Valve Control") was developed. The FORTRAN listing of the program is included in Appendix 1.

Input Requirements      The user must provide the following information, in addition to the usual input data of the Transients Program:

- 1) The coefficients of the transfer function  $K$ ,  $T_1$ ,  $T_2$ ,  $T_3$ ,
- 2) the operating mode of the converter, i.e. rectification on inversion,
- 3) the initial operating region on the converter control characteristic,
- 4) the commutating reactance  $X_c$ ,
- 5) the electrical frequency,
- 6) the connection of the converter transformer, i.e. wye-wye on wye-delta,
- 7) identification of a branch (usually a switch) where the reference direct current will be taken from,
- 8) three node names on the primary side of the converter transformer from which the commutation voltage of each valve will be calculated,
- 9) the limits  $V_{d \max}$ ,  $V_{d \min}$ , that are placed on the excursions of the regulator amplifier,
- 10) the pulse generator type.

Numerical Integration

The s-domain equation (2.4) can be expressed as two first order differential equations:

$$X(t) = \frac{d e_{\alpha}(t)}{dt}$$

$$e_{\alpha}(t) + T X(t) + P \frac{dX(t)}{dt} = KI(t) + KT_2 \frac{dI(t)}{dt} \quad (3.1)$$

where

$$I(t) = I_{ds} - I_d - \Delta I$$

$$T = T_1 + T_3$$

$$P = T_1 \cdot T_3$$

These equations, as described in more detail in the next section, represent the converter control loop when the regulator amplifier operates within the limits. They must be solved simultaneously with the rest of the external electric network. The numerical integration formula based on the trapezoidal rule was adopted in the program. This algorithm was chosen, firstly because it is the simplest second order implicit method and is numerically stable for any stepsize  $\Delta t$ <sup>17</sup>; secondly, it simplifies the interfacing problem as the Transients Program uses the same stepsize and integration technique. Applying the trapezoidal rule to equation (3.1) results in the algebraic difference equations

$$X(t) + X(t-\Delta t) = \frac{2}{\Delta t} [e_{\alpha}(t) - e_{\alpha}(t-\Delta t)]$$

$$\frac{1}{2} [e_{\alpha}(t) + e_{\alpha}(t-\Delta t)] + \frac{T}{2} [X(t) + X(t-\Delta t)] + \frac{P}{\Delta t} [X(t) - X(t-\Delta t)] \quad (3.2)$$

$$= \frac{K}{2} [I(t) + I(t-\Delta t)] + \frac{T_2 K}{\Delta t} [I(t) - I(t-\Delta t)]$$

Rearranging terms, this becomes

$$e_{\alpha}(t) = \frac{B}{A} I(t) + HIST(t-\Delta t)$$

$$X(t) = \frac{2}{\Delta t} [e_{\alpha}(t) - e_{\alpha}(t-\Delta t)] - X(t-\Delta t) \quad (3.3)$$

where

$$A = 1 + \frac{2T}{\Delta t} + \frac{4P}{(\Delta t)^2}$$

$$B = K(1 + \frac{2T}{\Delta t})$$

and the "history" of the state of the amplifier

$$\text{HIST}(t-\Delta t) = \frac{2K-B}{A} I(t-\Delta t) + \frac{A-2}{A} e_{\alpha}(t-\Delta t) + \frac{4P}{A \cdot \Delta t} X(t-\Delta t)$$

After the program enters the time-step loop, the instantaneous values of  $e_{\alpha}$  and  $X$  are calculated and the history term is updated at each step. Then the delay angles and the firing pulses are determined based on the equations described in the previous chapter.

The Interface      The electric network and the control system are solved separately in the Transients Program and in the subroutine VALCON, respectively. Variables such as ac bus voltages, dc line currents, valve status (open or close) etc., are passed from the main program to VALCON, which, after manipulation through its logic, returns the appropriate firing signals to continue the simulation. Modifications in the Transients Program to incorporate this interface are documented in Appendix 2 and a general flow chart of the simulation algorithm is shown in Fig. 3.1.



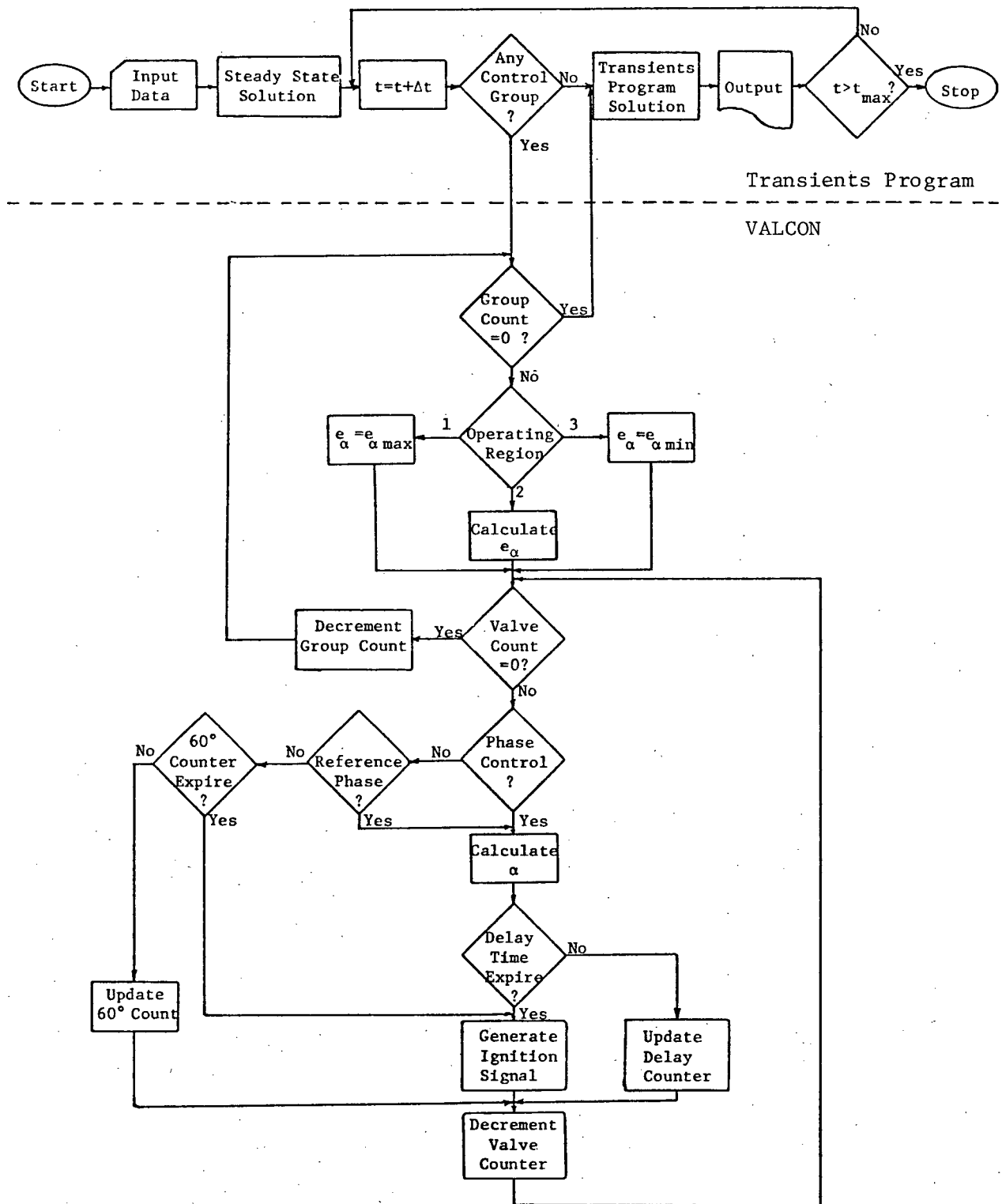


Fig. 3.1 Flow Chart of the Simulation.

### 3.2 Limiter Representation

The control amplifier output is usually clamped according to the maximum and minimum angle of delay constraints of the converters. This type of limiter creates a special problem of nonlinearity. The solution method which has been used in the existing simplified model is such that the derivatives of the output are set to zero<sup>7</sup> when a limit is reached, which changes the structure of the differential equations. To investigate the validity of this representation, the actual hardware arrangement of the control circuit must be analyzed. Assuming that all the transducers and filters are ideal, and neglecting all the protective circuits and monitoring devices, the control amplifier circuit is shown in Fig. 3.2. The overall relationship between the input and output voltage is<sup>18</sup>:

$$\frac{e_{\alpha}}{e_i} = -\frac{Z_0}{Z_i} \quad (3.4)$$

where  $Z_0$  = short-circuit transfer impedance function of the feedback loop

$Z_i$  = short-circuit transfer impedance function of the input circuit.

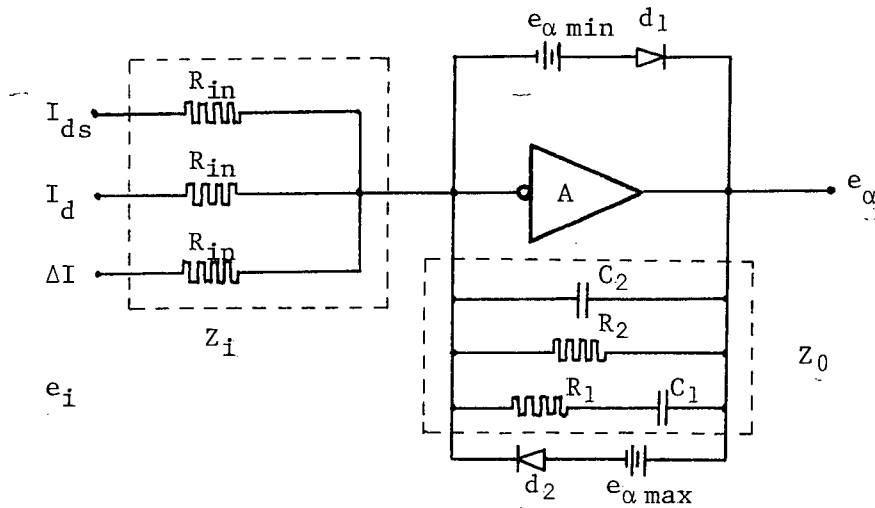


Fig. 3.2 Control Amplifier Circuit. A High Gain Amplifier; C, R's Capacitance and Resistance of the Damping Circuit;  $e_i$ ,  $e_{\alpha}$  Input & Output Voltages;  $d_1$ ,  $d_2$  clamping diodes.

The input transfer impedance  $Z_i$  is simply  $R_{in}$ , and the complex transfer impedance of the RC feedback network in terms of the Laplace transform operator  $S$  is in the same form as equation (2.5) with the time constants having the relationships given by<sup>19</sup>

$$\begin{aligned} T_2 &= R_1 C_1 \\ T_1 \cdot T_3 &= R_1 R_2 C_1 C_2 \\ T_1 + T_3 &= R_1 C_1 + R_2 C_2 + R_2 C_1 \end{aligned} \quad (3.5)$$

The function of the control amplifier can be divided into three different operating regions. Fig. 3.3 shows that in each region, the current relationship should be described by different differential equations:

- a)  $e_{\alpha \min} < e_{\alpha} < e_{\alpha \max}$  i.e. the amplifier is in its active region.  $e_{\alpha}$  varies as the input current  $i_1$  changes, the equation of the system
- $$e_{\alpha}(t) = -Z_0(t) i_1(t) \quad (3.6)$$
- b)  $e_{\alpha} = e_{\alpha \min}$  i.e. the amplifier is clamped to prevent it from going negative or less than minimum. The diode  $d_1$  is conducting and the output is kept at  $e_{\alpha \min}$ . When the amplifier is driven to the limit, the circuit will undergo a transient period which can be described by the equation

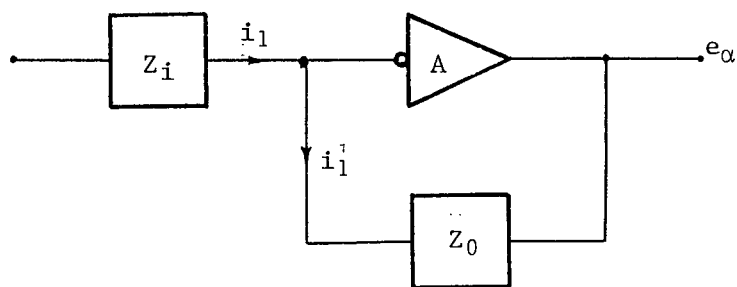
$$e_{\alpha \min} = Z_0(t) \cdot [i_2(t) - i_1(t)] \quad (3.7)$$

The amplifier comes out of the clamping condition when  $I_d$  becomes less than  $(I_{ds} - \Delta I)$ .

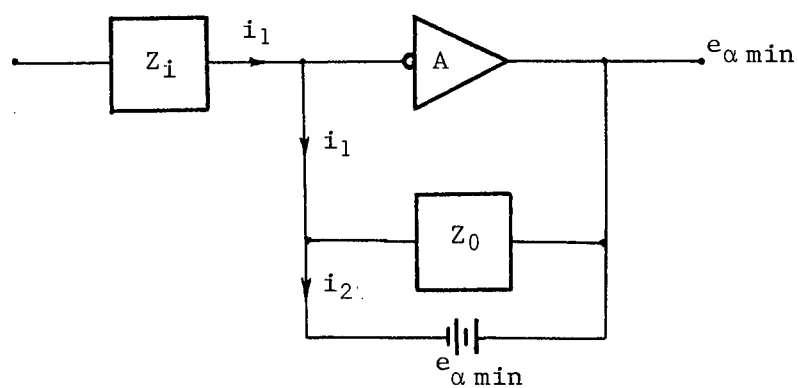
- c)  $e_{\alpha} = e_{\alpha \max}$  i.e. the amplifier goes into saturation or to a clamped value of maximum output. Diode  $d_2$  is conducting and the equation under this condition is

$$e_{\alpha \max} = Z_0(t) [i_2(t) - i_1(t)] \quad (3.8)$$

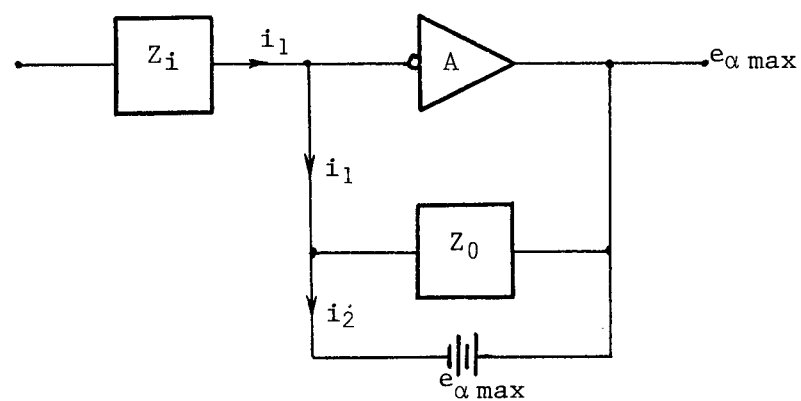
The amplifier comes out of this region when  $I_d$  becomes greater than  $(I_{ds} + \Delta I)$ .



(a)



(b)



(c)

Fig. 3.3 Three Operating Regions of the Control Amplifier: (a) - in active region; (b) - clamped to minimum value; (c) - clamped to maximum value.

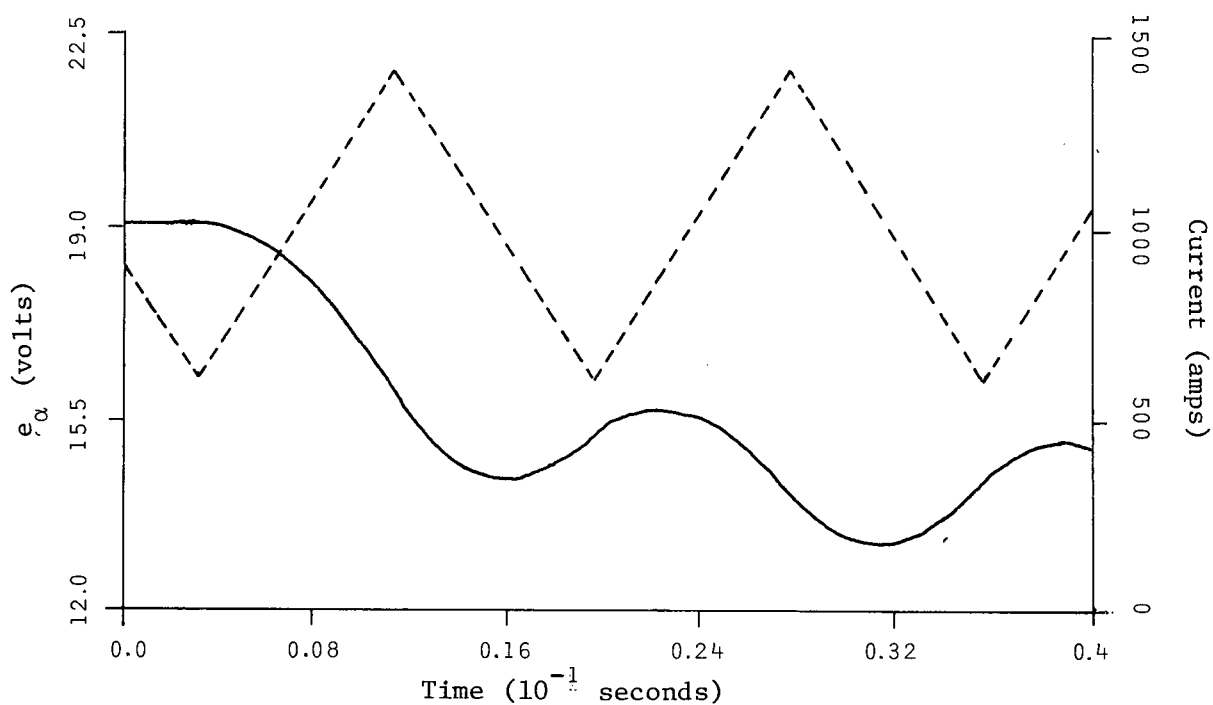
To simulate the behaviour of the amplifier accurately, all these three equations must be included. Every time the subroutine is called, the operating region of the amplifier is determined and the mathematical solution will be switched from one equation to another whenever the operating region is changed.

The previously used method of setting the derivatives equal to zero at the limit gives erroneous simulation results, especially when the system is subjected to disturbances which drive the amplifier in and out of the limit in short time intervals. To illustrate the difference between the two approaches, a simple control scheme, as shown in Fig. 2.4, was simulated with

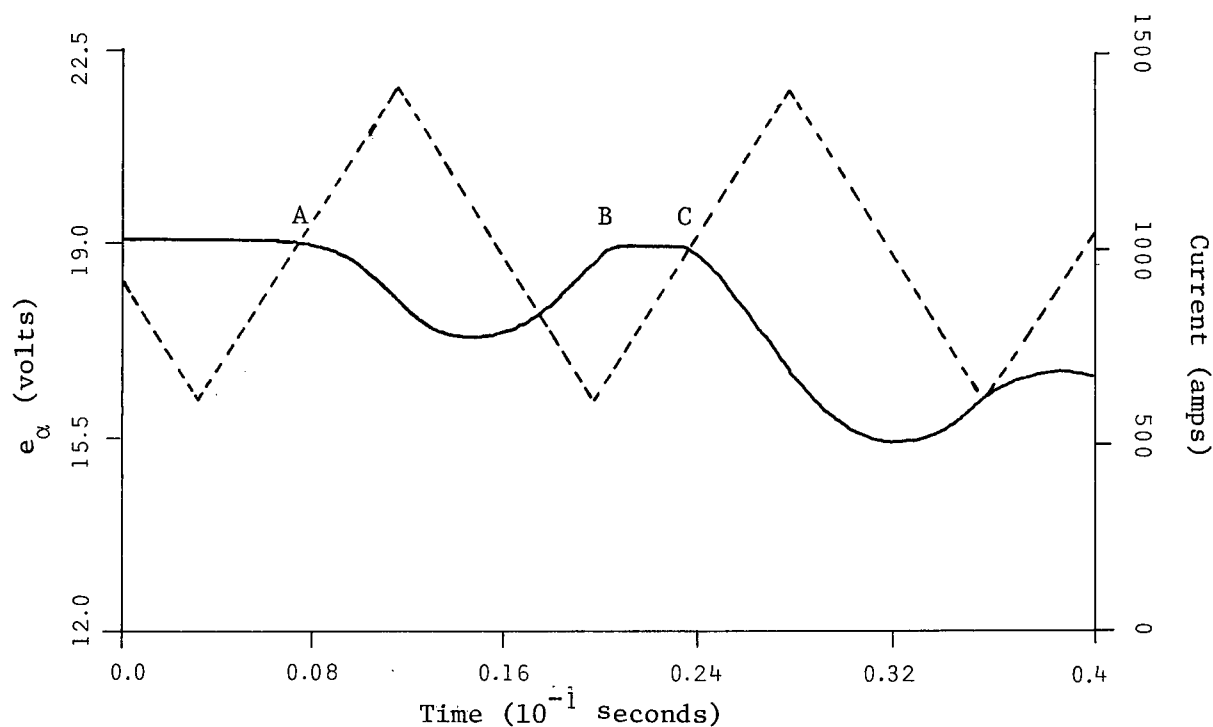
$$G(s) = \frac{1.39 (1 + 4.4s)}{(1 + .04s)(1 + .0103s)}$$

and  $I_{ds} = 900$  Amp.,  $\Delta I = -100$  Amp.  $e_{\alpha \max} = 18.9$  volt.

The converter operated in the upper limit in steady state and was subjected to a saw-tooth disturbance. Since  $I_{ds} - \Delta I = 1000$  Amp., the amplifier is expected to stay in the upper limit until the input current exceeds this value. Fig. 3.4(a) shows that the amplifier jumps out of the limit prematurely with the previously used approach, and thus cannot return to the limit again in the subsequent fall-off of the input current. The method of solving different differential equations according to the operating regions of the amplifier gives a more accurate simulation. Fig. 3.4(b) also shows that the amplifier responds differently depending on whether the amplifier has stayed in the limit long enough to reach its steady state: At A, the amplifier jumps out of the limit after the damping circuit reaches the steady state, while at C, the damping circuit is still in the transient process after the amplifier switches into the limit at B.



(a) First Approach : setting derivatives to zero when output hits the limit.



(b) Second Approach : solving different differential equations according to the operating regions of the amplifier.

Fig. 3.4 Response of the current regulator when subject to a saw-toothed disturbance : — amplifier output; - - - - current input.

### 3.3 Initialization

Typical transient studies start with the electric network being in its steady state conditions. While it is always possible to ramp the simulation up to steady state, this not only requires additional computer time, but also skill on the side of the user. It is therefore desirable to initialize the network variables to their steady-state values as closely as possible. The present version of the Transients Program has a subroutine which automatically calculates the ac steady state solution for a single source frequency. In addition, it has an option to read in user-specified initial data, which will override automatically computed values. The initialization process in the simulation of ac/dc system is complicated by the fact that such systems have two or more fundamental frequencies as well as harmonics, and that the converter valves create a discontinuity between the ac and dc components. Neither option mentioned is therefore adequate to handle the initialization alone. To solve the problem, a combination of the two features has been used.

At time  $t < 0$ , a typical system, as shown in Fig. 3.5, can be partitioned into three separate groups: The power transmitting ac system, the dc link, and the power receiving ac system. The converter bridges serve as the boundaries, and all the valves are assumed in open state at  $t < 0$ . With the ac networks disconnected from the dc system, dc voltages (simulated as ac sources of very low frequencies and amplitudes equal to the dc operating voltages) are inserted at the terminals of the dc line. AC sources are used because the steady-state subroutine can only handle ac steady-state solutions, since at dc, admittances of inductive branches would become infinite. Practice has shown that with a frequency of  $f = 10^{-3}$  Hz, the ac solution is sufficiently close to the dc solution<sup>14</sup>, and reactances  $\omega L$  and susceptances  $\omega C$

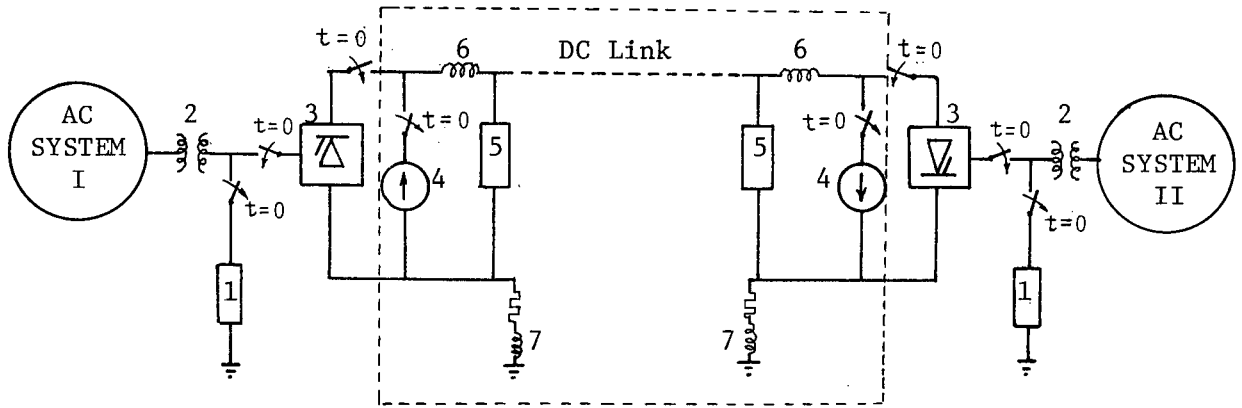


Fig. 3.5 System set up for initialization: 1 - Equivalent load; 2 - Converter transformer; 3 - Converter station; 4 - AC current source with very low frequency; 5 - DC filters; 6 - Smoothing reactor; 7 - Electrode line.

are still large enough to avoid numerical problems. This approach gives good dc steady state solution for the dotted area in Fig. 3.5, with all the harmonic components neglected.

To properly initialize the ac portions of the system, the dc network is represented as an equivalent load connected to each leg of the secondary windings of the converter transformers. The initial dc operating conditions, such as dc terminal voltages and currents, can be obtained from load flow studies, and with losses in the converter stations neglected, ac power equals dc power. The equivalent load, which will be a positive or negative impedance depending on whether the converter operates as rectifier or inverter, can be estimated from

$$Z_{eq} = \frac{V^2}{3S^*} \quad (3.9)$$

where  $V$  = the rms line-to-ground alternating voltage

$S^*$  = the conjugate of the apparent power.

With this load connected at  $t < 0$ , the initial conditions of the two ac systems are computed by the steady-state subroutine.

At  $t = 0$ , the equivalent loads are switched off and the ac and dc networks are reconnected through the valves. The dc steady-state initial



conditions are set through the read-in option, and with subroutine VALCON, determining which valves must be ignited, the system is virtually at its normal operating state and ready for the transient simulation for  $t > 0$ . Fig. 3.6 shows a simulation over a time span of 75 ms for a case of a six-pulse converter operation with both ac and dc filters. The system settles down very fast. Simulations with the order of dc and ac steady state solutions reversed were also studied and the results were basically identical. It is therefore reasonable to assume that harmonics can be ignored in the initialization.

Other researchers have found that ac/dc system simulations are very sensitive to wrong initial values<sup>12</sup>. One concern in the method described here is the behaviour of the valve dampers. Since the circuits in the converter bridge are disconnected during the computation of the steady-state solution, they are subjected to wrong initial conditions when the simulation starts at  $t = 0$ . Two cases were simulated: one with the simulation starting at the middle of the non-commutation period, i.e. the valve dampers are quiescent; the other with the simulation starting at a point of commutation, i.e. the valve dampers are in a transient state. The resulting curves in Fig. 3.7 show no differences after one sixth of a cycle. The exclusion of the valve dampers in the initialization process does not seem to cause noticeable disturbances.

However, improper initialization on any part of the dc line may give inaccurate results or even lead to wrong firing sequences. Fig. 3.8 illustrates the severity of this problem. The system studied previously is initialized in the same way except that the electrode line, which is simply modelled as a lumped R-L branch, was not included in the initialization, i.e. it had zero initial values. The curves show an erroneous high voltage

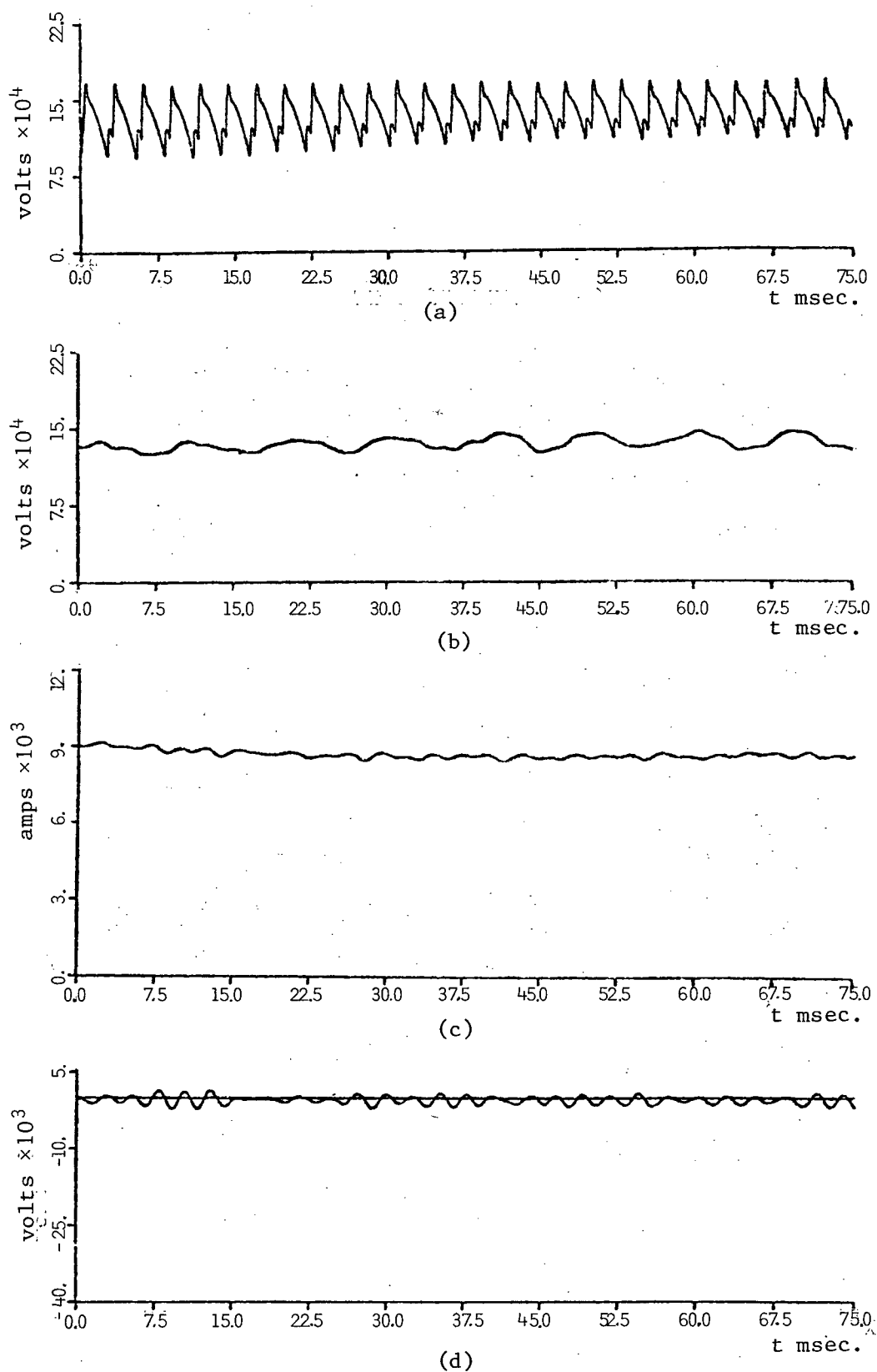


Fig. 3.6 Long run to verify steady state solution: (a) - Rectifier terminal voltage; (b) - DC line voltage; (c) - DC line current; (d) - Electrode line voltage.

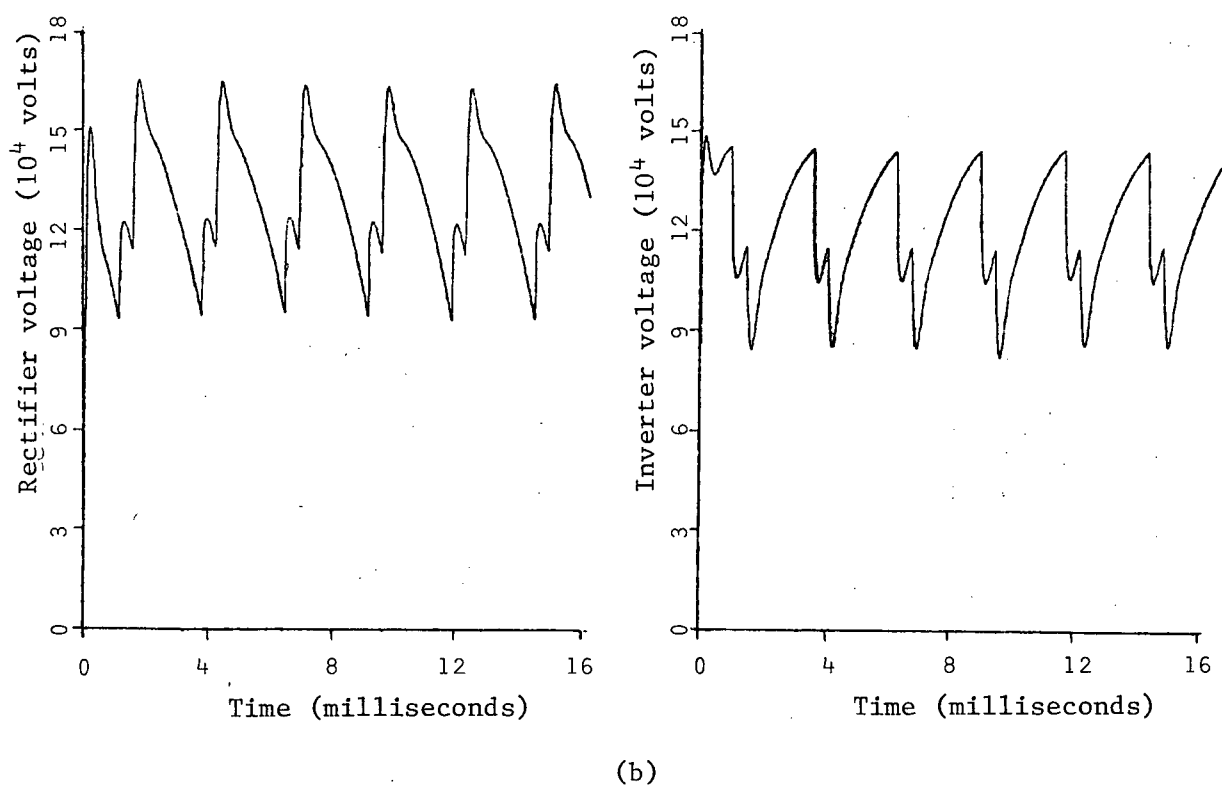
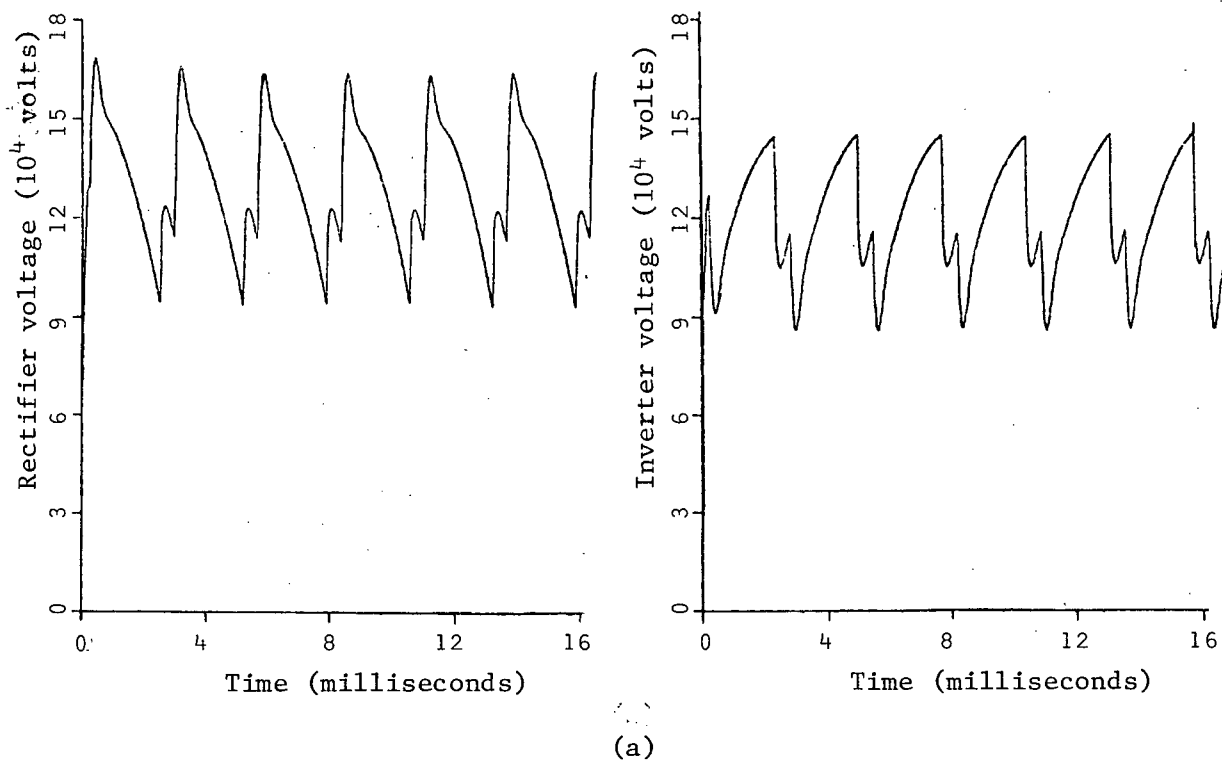


Fig. 3.7 Simulation with DC starts at (a) a point of commutation;  
(b) middle of non-commutation interval.

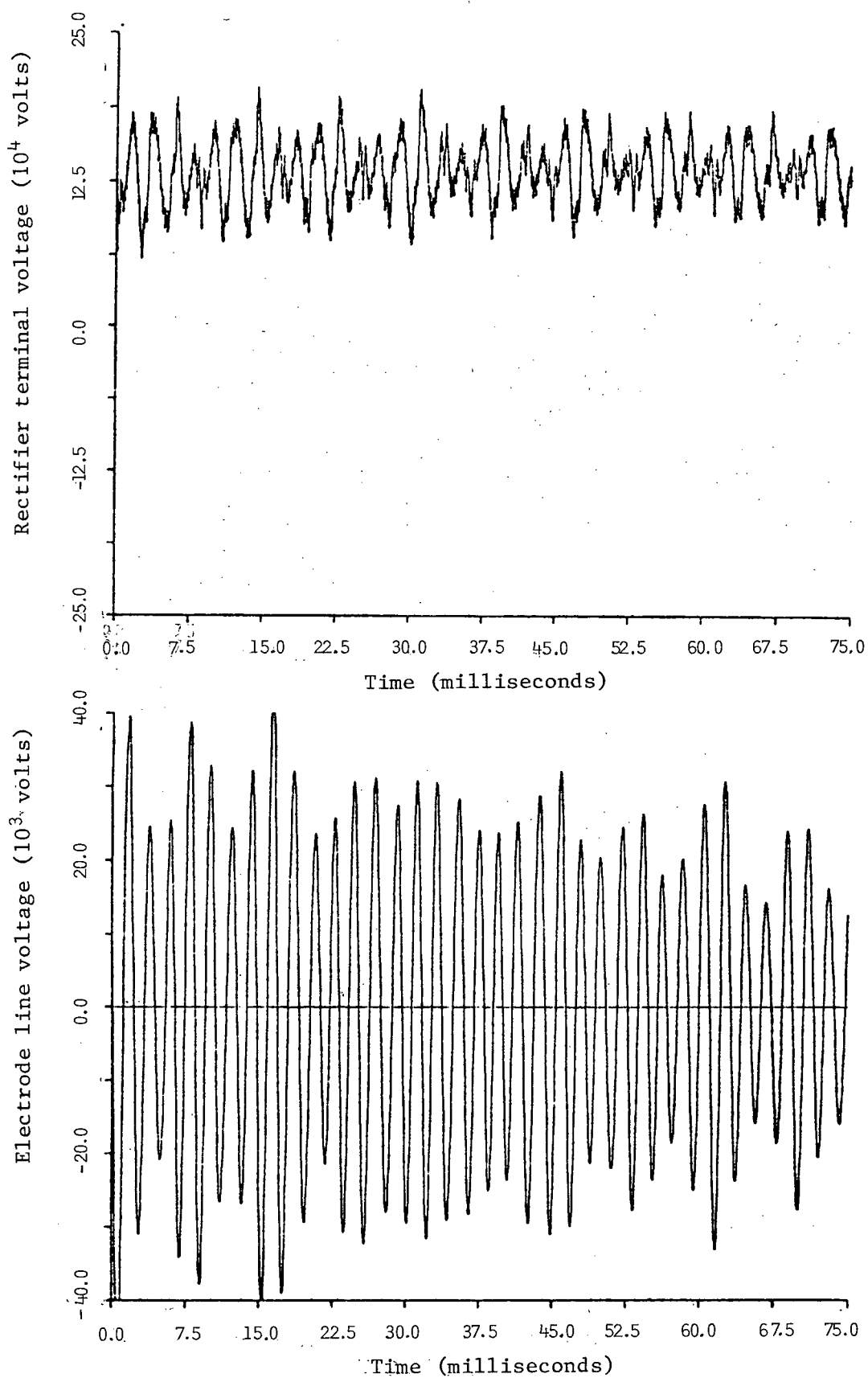


Fig. 3.8 Simulation results with electrode line starts at zero initial conditions.

oscillation on the electrode and an erroneous waveform at the converter terminal. The simulation does not settle to steady-state even after a few cycles. Since most ac/dc system simulations consist of a large number of components, the initialization process described must be done with extraordinary care. It is believed that with some program changes in the steady-state subroutine to handle the superposition of solutions at different network frequencies, the whole initialization process could be done automatically. This is beyond the scope of this thesis, and a possibility for future improvements.

#### 4. HARMONIC ANALYSIS

One advantage of a detail converter model is its ability to simulate the interaction between the ac and dc sides of the network accurately. This is important both in steady-state and transients analysis. One major criterion in HVDC system design is its harmonic performance. The appearance of undesirable harmonics<sup>13,20</sup> may cause overheating of capacitors and generators, interference in telecommunication circuits, shortened life of incandescent lights, instabilities of the converter control, and remote resonances in the ac system. Corrective measures must be imposed to eliminate them at the source or at least to reduce them to permissible levels. A good amount of published literature describes the different methods for determining the level of harmonic generation which can be anticipated from a converter installation. The main objective of this chapter is not to discuss these laborious mathematical procedures in detail, but rather to show the usefulness of the digital time-domain simulation in predicting the harmonic behaviour, and to compare the results with those obtained from the theoretical calculations where appropriate.

##### 4.1 Analyzing Method

A Fourier Analysis Program was used to analyze the simulation results. The output quantities of the Transients Program (node voltages, branch currents, branch voltages, etc., as a function of time) can be stored in a file for further processing. Once the simulation settles into steady-state, the values within one period can be expressed as

$$f(x) = \sum_{i=0}^{\infty} a_i \cos(ix) + \sum_{i=0}^{\infty} b_i \sin(ix) \quad (4.1)$$

where  $a_i$ ,  $b_i$  are the coefficients of the Fourier series.

The program, originally written by H.W. Dommel<sup>21</sup>, reads all the  $n$  data points within a user-specified period and computes the cosine coefficients  $a_0 \dots a_m$  and sine coefficients  $b_0 \dots b_m$  of equation (4.1) as well as the magnitude of

$$C_i = \sqrt{a_i^2 + b_i^2} \quad (4.2)$$

with

$$i = 0, 1, \dots, m$$

$$m = \frac{n}{2}, \text{ when } n \text{ is even}$$

$$m = \frac{n-1}{2}, \text{ when } n \text{ is odd}$$

The resulting finite series

$$F(x) = \sum_{i=0}^m a_i \cos(ix) + \sum_{i=0}^m b_i \sin(ix) \quad (4.3)$$

will pass through each data point of the specified period, and provide a smooth interpolation between points with the least number of harmonics. A FORTRAN listing of the program is shown in Appendix 3.

In order to obtain higher order harmonics, the time step for the simulation must be chosen in such a way that the computation cost does not increase unnecessarily on one hand, and that the results are still accurate enough on the other hand. Experience has shown that for analyzing characteristic harmonics, a sampling rate of 10 points per cycle at the highest frequency of interest will give reasonable solutions. In studying imbalance factors, however, a step length of less than one degree of fundamental frequency should be used.

## 4.2 Harmonic Contents

A converter bridge will produce to some noticeable degree all the lower order harmonics. These harmonic currents appear in both the ac and dc networks, and may penetrate into the power system far from the connection point. Under normal operating conditions, some harmonics are predominant in magnitude. They are usually referred to as normal or characteristic harmonics and attract most of the attention in system design. They are of the following order:

$$\text{DC side} \quad \therefore \quad h = kp$$

$$\text{AC side} \quad \therefore \quad h = kp \pm 1$$

where

$$h = \text{order of a harmonic}$$

$$k = \text{pulse number}$$

$$p = 1, 2, 3 \dots \text{any positive integer}$$

Based on the assumptions of perfectly smoothed direct current (i.e. infinite smoothing inductance on the dc side) and symmetrical operation of the ac network, the amplitude of the characteristic ac side current harmonics for overlap angles of less than  $60^\circ$  may be written as<sup>13, 14</sup>:

$$I_h = \frac{I_{10} F_1}{hD} \quad (4.4)$$

where

$$I_{10} = \text{rms fundamental alternating current with no overlap}$$

$$D = \cos \alpha - \cos (\alpha + u)$$

$$U = \text{overlap angle}$$

$$F_1 = [A^2 + B^2 - 2AB \cos (2\alpha + u)]^{\frac{1}{2}}$$

$$A = \frac{\sin [(h-1) u/2]}{h-1}$$

$$B = \frac{\sin [(h+1) u/2]}{h+1}$$



and the rms value of the harmonics of the direct voltage is given by

$$V_{dh} = V_{do} F_2 \quad (4.5)$$

where

$$F_2 = [C^2 + D^2 - 2CD \cos (2\alpha + u)]^{1/2}$$

$$C = \frac{\cos [(h-1) u/2]}{h-1}$$

$$D = \frac{\cos [(h+1) u/2]}{h+1}$$

These equations are for idealized conditions, and the true value will vary from the results obtained with them depending on the operating condition of the particular system. In the past, planning engineers computed these ideal harmonic levels and used empirical values based on the contractor's experience of previous HVDC installations to make modifications<sup>22</sup>. As this discussion progresses, the practicality of the simplifying assumptions will be investigated.

The first questionable assumption is the perfect smoothness of direct current. In reality, the smoothing reactors in HVDC installations are typically in the range of 0.5 to 1.0 H. Table 4.1 compares the harmonics contained in the simulated current curve with two theoretical calculations, one based on equation (4.4) and another derived earlier by Brown and Smith<sup>23</sup> who described the current wave shape on the ac side of the mercury arc rectifier under pure resistive load condition as:

$$i = \frac{3.308 I_d}{\pi} [\sin \theta - 0.226 \sin 5\theta - 0.113 \sin 7\theta + 0.091 \sin 11\theta + 0.065 \sin 13\theta - 0.0567 \sin 17\theta \dots] \quad (4.6)$$

The harmonics extracted from the digital simulation lie in between the two extremes. Furthermore, a finite inductance also implies that the current wave shape is affected by the nature of the load. Simulated values of ac

ORDER OF HARMONIC	MAGNITUDE OF HARMONIC CURRENT			
	Calculation based on $L=0$	EMTP Simulation Results		Calculation based on $L=\infty$
		$L = .5H$	$L = 1H$	
1	1.000	1.000	1.000	1.000
5	.226	.202	.198	.192
7	.113	.131	.135	.132
11	.091	.079	.080	.074
13	.065	.065	.067	.057
17	.0567	.0404	.0427	.0354
19	.0454	.0339	.0352	.0273
23	.0412	.0183	.0207	.0153
25	.0349	.0139	.0148	.0108

Table 4.1 Comparison of current harmonics obtained from theoretical calculations and from Fourier analysis of simulated curves.

characteristic harmonic currents as a function of direct current are given in Fig. 4.1. The overlap angle, which results from the commutating reactance, affects the harmonic content as the loading condition changes. This should be taken into account in the optimal design of the filters, the converter transformers and the smoothing reactors.

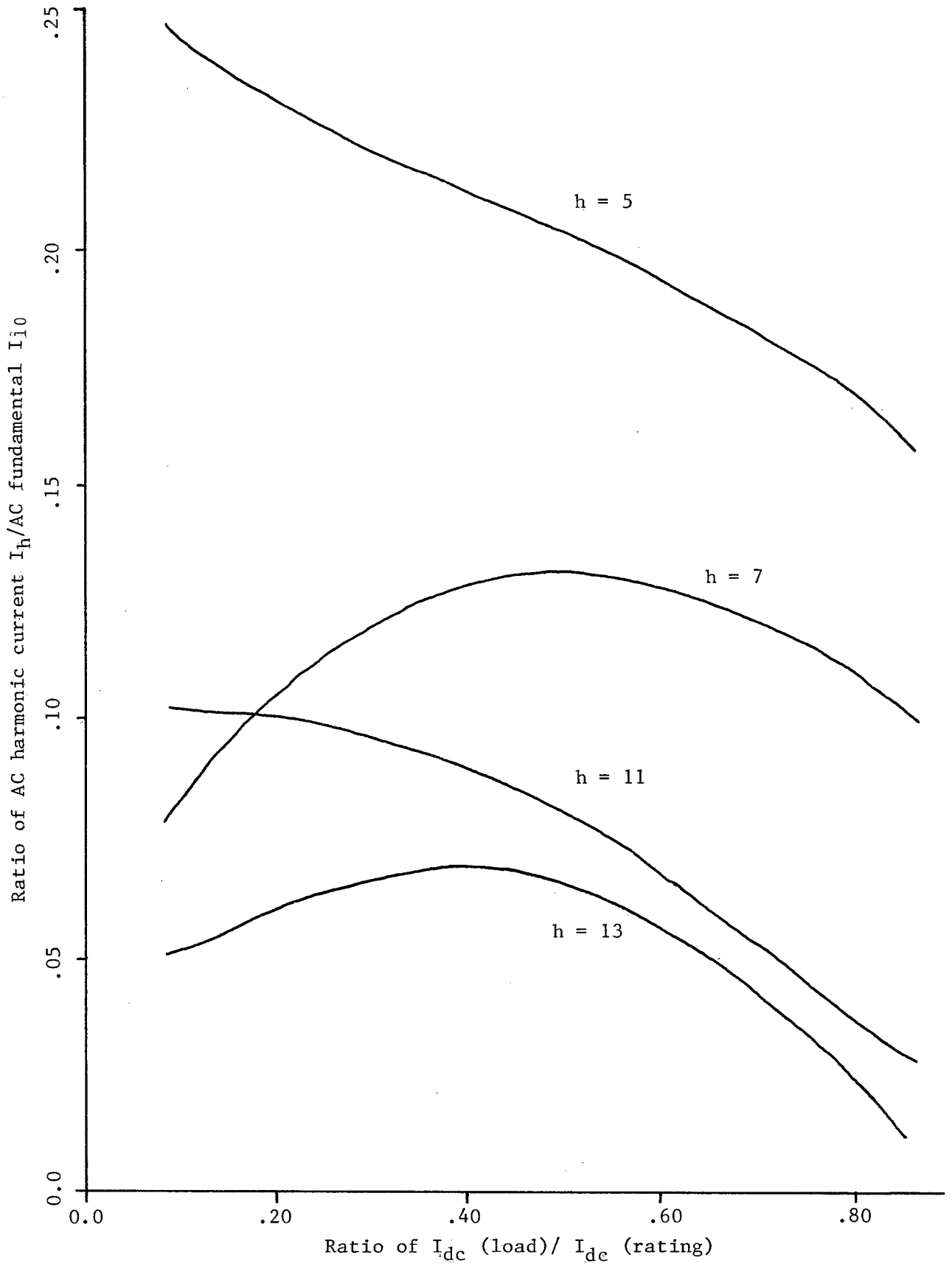


Fig. 4.1 Simulated AC Characteristic Harmonic Current for 6-pulse Operation.

### 4.3 Abnormal Harmonics

The assumption of ideal balanced (symmetrical) operation is also not realistically achievable. Asymmetrical conditions include<sup>25,26</sup> firing angle errors from converter control, distortions of the ac bus voltage waveforms, imbalances in the ac system voltages and unequal transformer phase impedances. These imperfections result in the generation of non-characteristic or abnormal harmonics. The effect of imbalances in the ac system voltages on the dc harmonics was studied. Table 4.2 contains the magnitude of the harmonic voltages on the dc side due to imbalance in the voltage of one phase of the ac bus. The imbalances in magnitude and phase angle are -5% of the nominal value. Results show that the characteristic harmonics do not change much but an appreciable amount of even harmonics are generated. These agree with the findings of Mathur and Sharaf<sup>24</sup>. In practical systems, a certain degree of different imbalance factors is inevitable. Most imbalances result from an interaction among various phenomena. For example, one or more phases of the ac voltages can be depressed as a result of a remote fault, which will lead to the generation of certain abnormal harmonics. These harmonics will propagate into the ac system, which in turn may lead to voltage distortion. Such cumulative effects cannot be described by simple mathematical formulations. The Transients Program is capable of simulating cases with combinations of imbalance factors. For example, a situation where the supplying ac voltages are at  $1.0/-90^\circ$  ,  $.98/151.2^\circ$  ,  $1.02/31.2^\circ$  p.u., has been analyzed. Fig. 4.2 shows that the magnitudes of some non-characteristic harmonics are comparable to those of the characteristic ones in this case.

There is no doubt that this simulation approach for obtaining non-characteristic harmonics offers a relatively easy and economical way to gain a deeper and more systematic understanding of the causes and effects in the

HARMONIC ORDER	RECTIFIER SIDE			INVERTER SIDE		
	Balanced Operation	Imbalance of AC		Balanced Operation	Imbalance of AC	
		Magnitude	Phase		Magnitude	Phase
1	.0000	.0017	.0018	.0009	.0007	.0021
2	.0033	.0208	.0375	.0019	.0172	.0381
3	.0015	.0019	.0020	.0008	.0008	.0005
4	.0007	.0084	.0148	.0008	.0059	.0081
5	.0007	.0015	.0004	.0022	.0022	.0016
6	.1479	.1394	.1463	.1519	.1469	.1522
7	.0025	.0034	.0023	.0046	.0044	.0048
8	.0007	.0104	.0191	.0024	.0115	.0176
9	.0019	.0027	.0014	.0005	.0004	.0001
10	.0010	.0065	.0106	.0004	.0031	.0056
11	.0016	.0034	.0018	.0004	.0004	.0003
12	.0472	.0413	.0446	.0439	.0395	.0440
13	.0017	.0028	.0021	.0004	.0002	.0013
14	.0012	.0072	.0113	.0011	.0052	.0086
15	.0015	.0029	.0009	.0006	.0005	.0003

Table 4.2 Comparison of dc voltage harmonics under balanced operation and imbalance in magnitude and phase in one phase of the ac bus.

generation of harmonics on the ac and dc side of converters. Moreover, current and voltage loadings in each element of the filter arms are readily available, which are valuable to the engineers who must select the protective level of these devices.

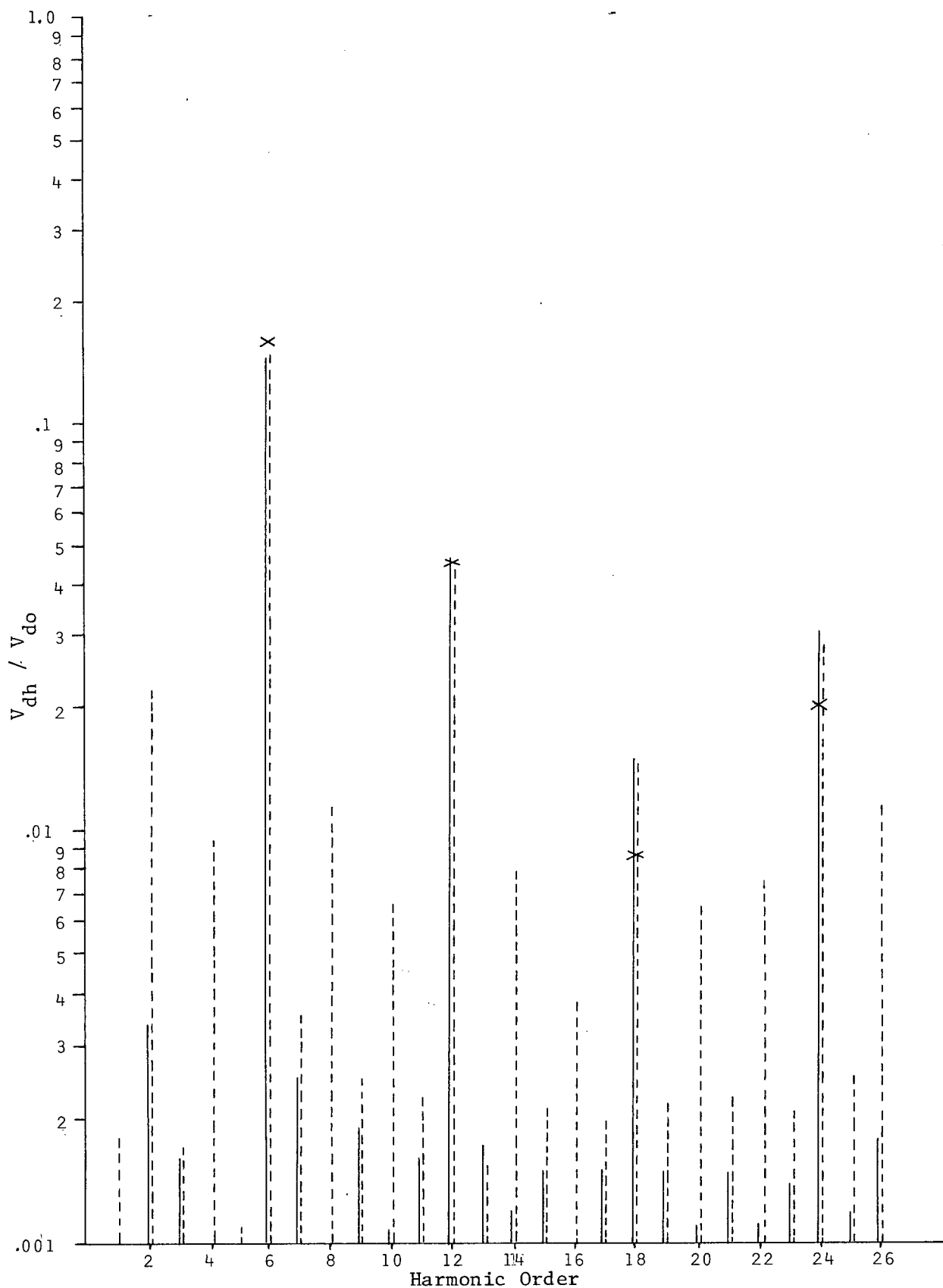


Fig. 4.2 Harmonic voltage on the dc side of the rectifier terminal:  
 — balance operation; --- imbalance operation;  
 × level of characteristic harmonics calculated by equation (4.5).

## 5. TRANSIENTS SIMULATION

Two examples are presented in this chapter to test the capability of the converter model in transients simulations. Part of the network from the Pacific HVDC Intertie System is used. The transmission line data and the converter equipment layout of the system is included in Appendix 4.

### 5.1 Point to Point Operation

As a preliminary test, a simple two terminal case was studied. Results using the simplified model mentioned in Chapter 1 were used as a reference. The simplified model was developed in the early 1970's<sup>27</sup> for studies connected with DC circuit breaker tests. It simulates the HVDC converter station as a dc voltage source whose amplitude is controlled by its current output. With this simplified model, the ac networks and the converter transformers are totally ignored and the valve and anode dampers are represented as an R C-branch in parallel with the dc source. In the detailed case, the system configuration is similar to Fig. 2.1. The ac side behind each converter is represented as ac voltage sources behind Thevenin equivalent impedances, whose values can be found from the positive and zero sequence short-circuit MVA. The converter transformers are connected as wye grounded/wye and the valve and anode dampers are represented in detail. The dc line is 850 miles long and operates in monopolar ground return mode. A line-to-ground fault was applied 50 miles from the rectifier end at time  $t = 10$  msec. The voltage and current at the rectifier terminals are shown in Fig. 5.1 for both types of models (see Appendix 5 for the input listings of both runs). The agreement is reasonably good. The phase shift between the two curves may be due to the exclusion of ac circuits and the lumped

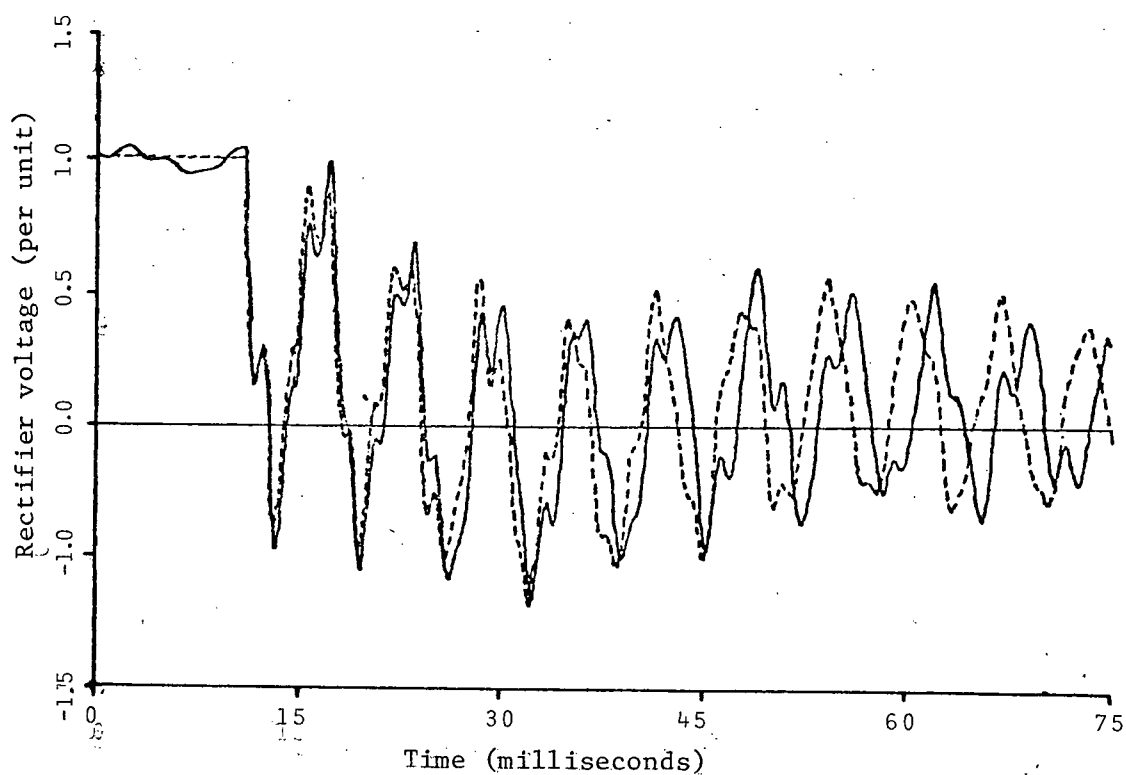
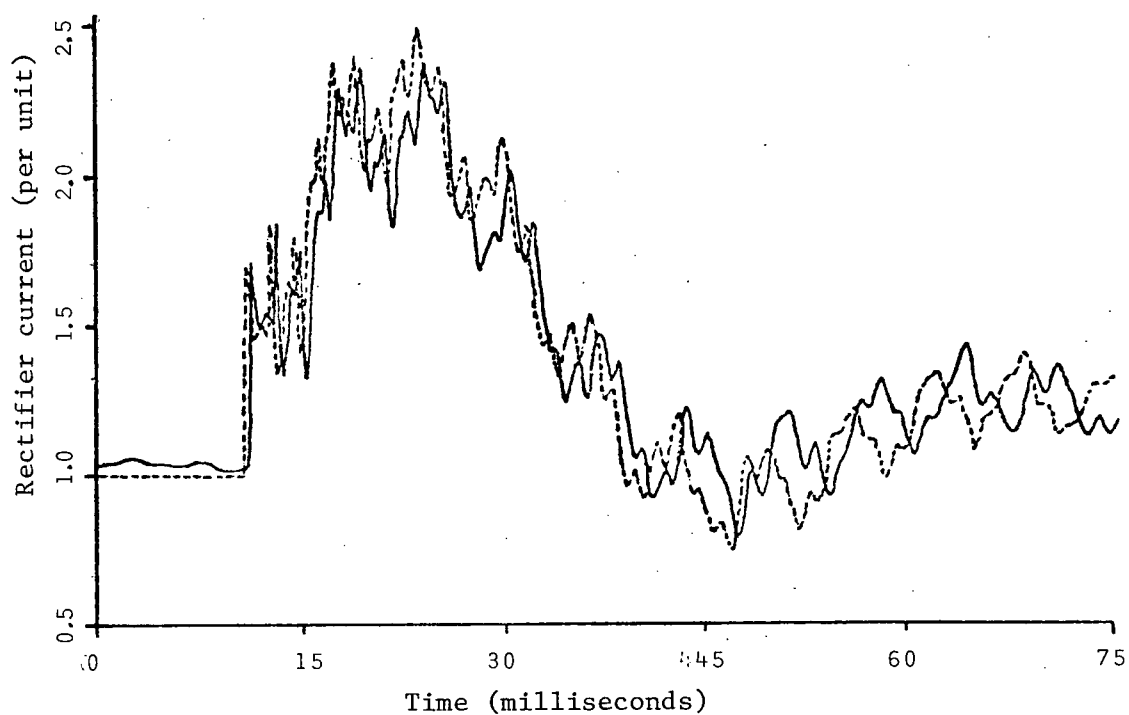


Fig. 5.1 Comparison between simplified and detailed converter station models for a fault on the dc line. Solid line = detailed model; dotted line = simplified model.



representation of dampers in the simplified simulation. In such simple cases, the simplified model does save computation time, while the detailed model provides more insight into the stress on the conversion components and the interaction between the ac and dc sides.

## 5.2 Three-Terminal Operation

To check the performance of a prototype dc circuit breaker in the field, several tests were conducted on the Pacific HVDC Intertie System<sup>8,15</sup>. The system was tapped as a three-terminal system with constant voltage rectifier control and independent constant current controls on the two inverters. The network set-up is shown in Fig. 5.2, and the system steady-state conditions before the staged fault test are summarized in Table 5.1.

Two manually-initiated faults were applied, a close-in fault by operating an ac breaker which was connected to ground through a  $5\Omega$  resistor, and a remote fault by dropping a wire pendulum to short the pole conductor to a tower at 250 miles away from the breaker. Melvold et al.<sup>15</sup> made some comparisons between field tests and computer simulations using the simplified model. The same arrangement was simulated using the detailed model. A sample data deck of the simulation is included in Appendix 6. The resulting curves were superimposed with the results given in reference [15]. As seen in Fig. 5.3 and 5.4, closer agreement with the field test measurements can be obtained using the detailed model. The converters were operated with abnormally large valve voltage stresses resulting from the large commutation margins. Totally ignoring the effects of the ac circuits in the simplified simulation may cause the inaccurate prediction of the current transfer among the terminals. Furthermore, the slight disagreement between the field tests and the detailed simulation, primarily in the form of high frequency oscil-

CELILO

SYLMAR

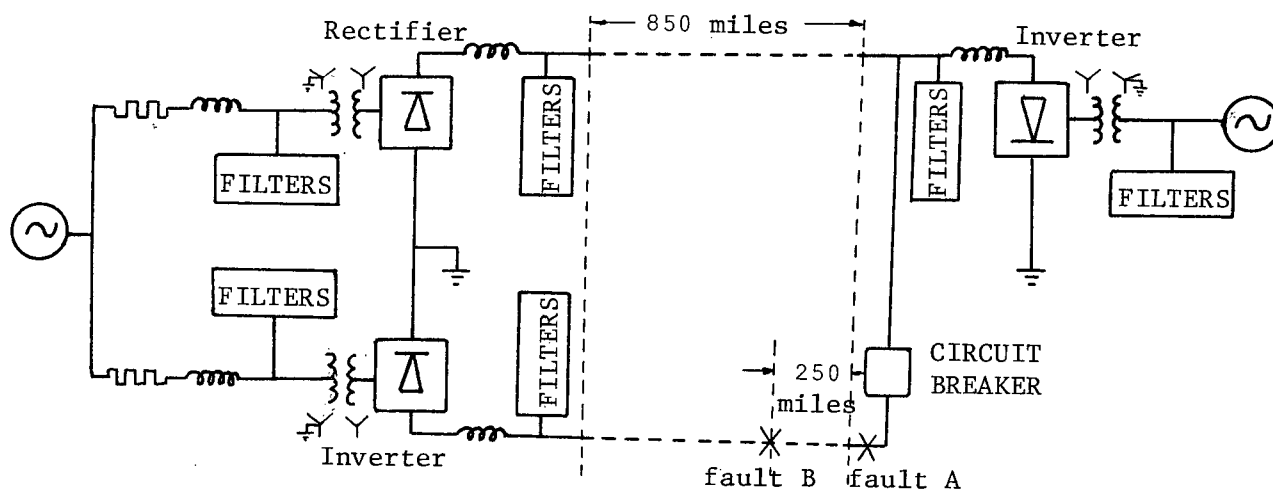


Fig. 5.2 System Configuration for DC Circuit Breaker Test

FAULT	CELILO RECTIFIER	SYLMAR INVERTER	CELILO INVERTER
CLOSE-IN	69.2KV/630A	63KV/330A	53.2KV/350A
REMOTE	70.5KV/558A	60KV/290A	50.5KV/306A

TABLE 5.1 Steady-State System Parameters Before Fault

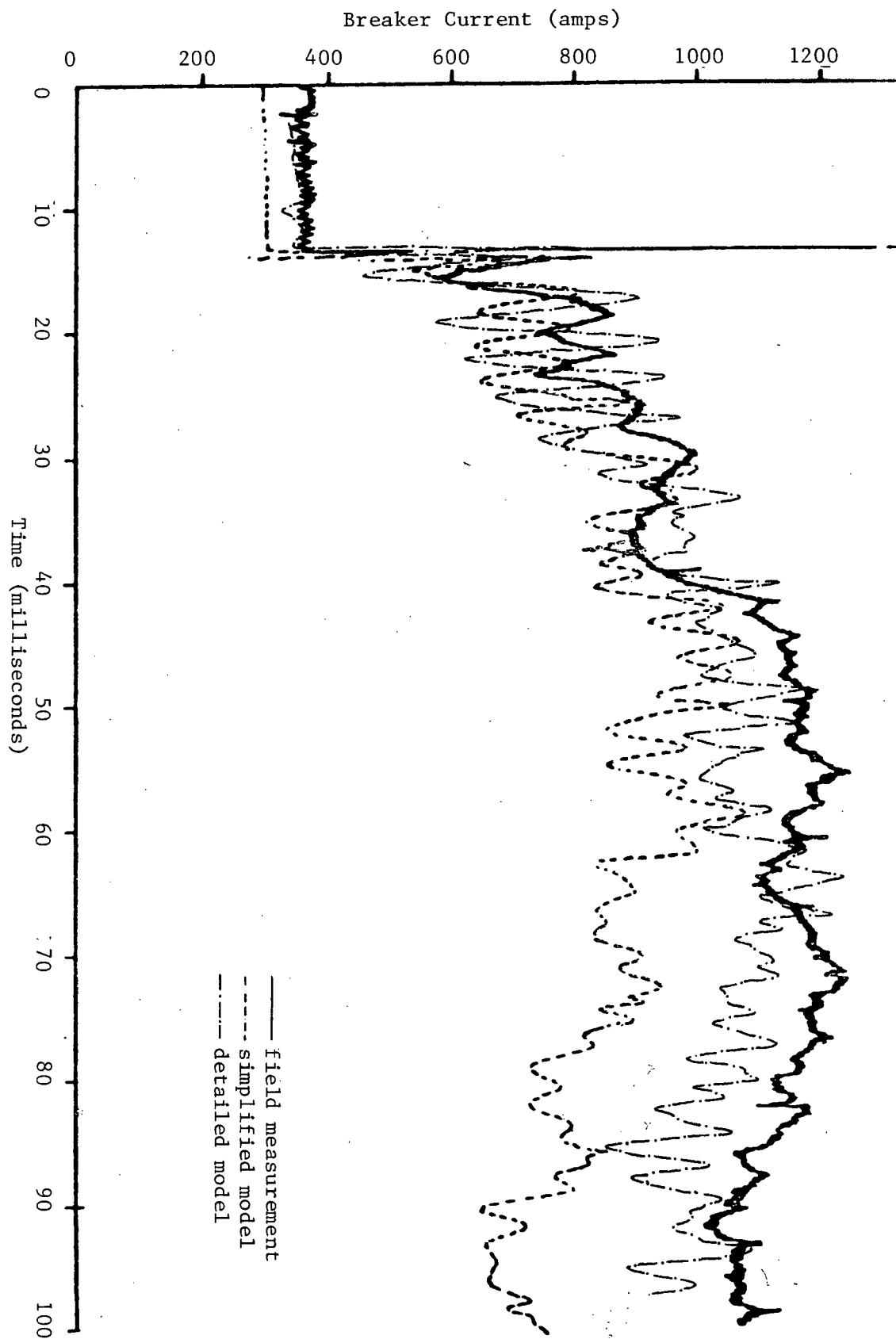


Fig. 5.3 Current through dc breaker following a close-in fault.

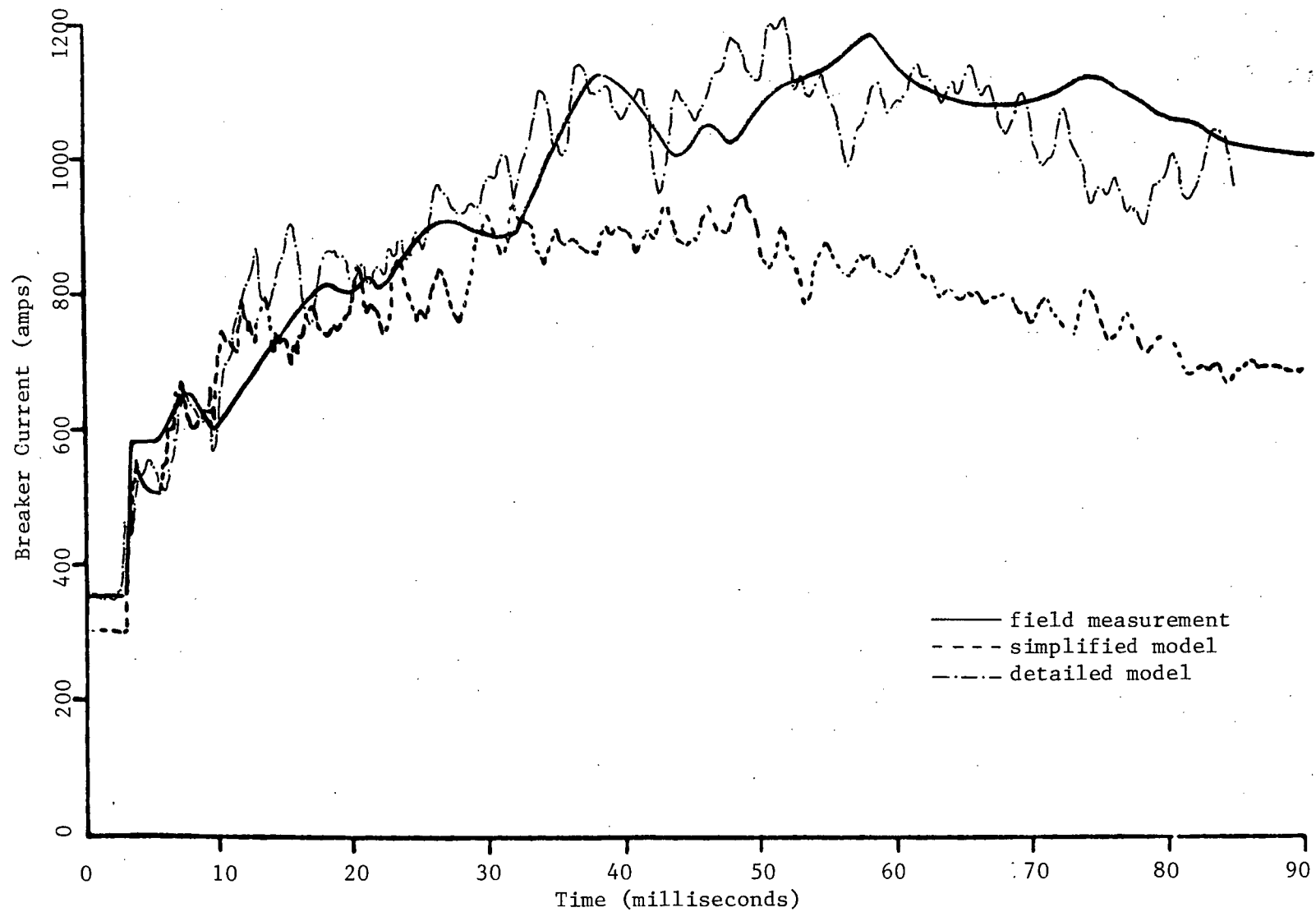


Fig. 5.4 Current through dc breaker following a remote fault.

lations, may be attributed to the inability to represent the frequency dependence of line parameters in the UBC version of the Transients Program.

## 6. CONCLUSIONS

This thesis describes the development of a new converter model which allows the user to represent HVDC converter valves and their associated firing control systems in the UBC version of the Electromagnetic Transients Program. The modified program can be used to simulate interactions between the ac and dc side and the behaviour of the control system for any type of steady-state or transient operating condition.

The new model takes account of the actual hardware arrangement of the control amplifier which leads to a more accurate representation of the limiters. Efforts have been made to minimize unnecessary computations in the initialization process. The method developed in this thesis is very economical, but it could be improved and made more or less foolproof if the whole procedure were done automatically. This would be a worthwhile topic for future investigations.

The model was applied to harmonic steady-state analysis and transient analysis to verify its capability. In the latter application, simulation results came close to field measurements. However, it should be realized that the frequency-dependent characteristics of line parameters had been neglected in these studies. Considering the complex frequency spectra associated with the harmonics and transients, this would definitely contribute some inaccuracies in the simulation. Modelling of frequency-dependent parameters is the subject of an ongoing Ph.D. project in this Department, and therefore beyond the scope of this M.A.Sc. thesis.

In terms of complexity, capability and flexibility, this model lies in between the simplified dc source model and the 'TACS' package<sup>7</sup>. It

is adequate and particularly useful for basic studies in the research environment of a university. The model is developed not as a substitute to either of the two existing features but as a supplement to these.

## REFERENCES

- [ 1] Allan Greenwood, "Electrical Transients in Power Systems", Wiley-Interscience, 1971.
- [ 2] H.W. Dommel, "Digital Computer Solution of Electromagnetic Transients in Single- and Multiphase Networks", IEEE Trans. on PAS, Vol. PAS-88, pp. 388-396, April 1969.
- [ 3] J.E. Hudson, E.M. Hunter and D.D. Wilson, "EHV-DC Simulator", IEEE Trans. on PAS, Vol. PAS-85, pp. 1101-1107, Nov. 1966.
- [ 4] S. Sasaki, H. Matsubara and D.J. Melvold, "High-Accuracy Analysis of Fault Surge by DC-TNA on HVDC Transmission Lines and Comparison with Field Test Results", Paper submitted to 1980 IEEE-PES Summer Meeting.
- [ 5] J.P. Bickford, N. Mullineux and J.R. Reed, "Computation of Power-System Transients", Peter Peregrinus Ltd., 1976.
- [ 6] H.W. Dommel, I.I. Dommel, "Transients Program User's Manual", U.B.C. Vancouver, 1976.
- [ 7] L. Dube, H.W. Dommel, "Simulation of Control Systems in an Electromagnetic Transients Program with TACS", IEEE PICA Conference, pp. 266-271, May 1977.
- [ 8] G.A. Hofmann, G.L. LaBarbera, N.E. Reed, L.A. Shillong, W.F. Long and D.J. Melvold, "Field Test of HVDC Circuit Breaker: Load Break and Fault Clearing on the Pacific Intertie", IEEE Trans. on PAS, Vol. PAS-95, pp. 829-838, May/June 1976.
- [ 9] D. J. Melvold, P.C. Odam and J.J. Vithayathil, "Transient Overvoltages on an HVDC Bipolar Line During Monopolar Line Faults", IEEE Trans. on PAS, Vol. PAS-96, pp. 591-601, 1977.
- [10] H.W. Dommel and W.S. Meyer, "Computation of Electromagnetic Transients", Proc. IEEE, Vol. 62, pp. 983-993, July 1974.
- [11] H.W. Dommel, "Nonlinear and Time-varying Elements in Digital Simulation of Electromagnetic Transients", Proc. 1971 PICA Conference, pp. 121-127, Boston, Mass., May 1971.
- [12] J. Arrillaga, J.G. Campos Barros and H.J. Al-Khashali, "Dynamic Modeling of Single Generators Connected to HVDC Converters", IEEE Trans. on PAS, Vol. PAS-97, pp. 1018-1029, July/Aug. 1978.
- [13] E.W. Kimbark, "Direct Current Transmission", Vol. 1, Wiley-Interscience 1971.
- [14] E. Uhlmann, "Power Transmission by Direct Current", Springer-Verlag, 1975.



- [15] J. Melvold, P.R. Shockley, W.F. Long and N.G. Hingerani, "Three Terminal Operation of the Pacific HVDC Intertie for DC Circuit Breaker Testing", IEEE Trans. on PAS, Vol. PAS-95, pp. 1287-1296, July/Aug. 1976.
- [16] J.D. Ainsworth, "The Phase-locked Oscillator - A New Control for Controlled Static Converters", IEEE Trans. on PAS, Vol. PAS-87, pp. 859-865, March 1968.
- [17] C.W. Gear, "Numerical Initial Value Problems in Ordinary Differential Equations", Prentice-Hall Inc., 1971.
- [18] W.J. Karplus, W.W. Soroka, "Analog Methods - Computation and Simulation", McGraw-Hill, 1959.
- [19] F.R. Bradley, R. McCoy, "Driftless D-C Amplifier", Electronics, Vol. 25, pp. 144-148, April 1952.
- [20] D.J. Melvold, "Pacific HVDC Intertie System AC Side Harmonic Studies", IEEE Trans. on PAS, Vol. PAS-92, pp. 690-701, March/April 1973.
- [21] H.W. Dommel, "Case Studies on Electromagnetic Transients", 1978.
- [22] J.J. Vithayathil, D.J. Melvold and V. Madzarevic, "Calculation and Measurement of Harmonics on the AC side of Converter Stations of the Pacific HVDC Intertie", Proc. on Symposium on HVDC Power Transmission, pp. 269-324, 1976.
- [23] H.D. Brown, J.J. Smith, "Current and Voltage Wave Shape of Mercury Arc Rectifiers", AIEE Trans., Vol. 52, pp. 973-986, 1933.
- [24] R.M. Mathur and A.M. Sharaf, "Harmonics on the DC side in HVDC Conversion", IEEE Trans. on PAS, Vol. PAS-96, pp. 1631-1638, Sept./Oct. 1977.
- [25] T. Subbarao and J. Reeve, "Harmonics Caused by Imbalanced Transformer Impedances and Imperfect Twelve-pulse Operation in HVDC Conversion", IEEE Trans. on PAS, Vol. PAS-95, pp. 1732-1735, Sept./Oct. 1976.
- [26] J. Reeve and P.C.S. Krishnayya, "Unusual Current Harmonics Arising from High-Voltage DC Transmission", IEEE Trans. on PAS, Vol. PAS-87, pp. 883-893, March 1968.
- [27] W.F. Long, "A Study on Some Switching Aspects of a Double Circuit HVDC Transmission Line", IEEE Trans. on PAS, Vol. PAS-92, pp. 734-741, March/April 1973.

## APPENDIX 1

## Subroutine VALCON Programme Listings

```

1  SUBROUTINE VALCON(ISTEP, DELTAT, KSWTCH, KPOS3)
2  COMMON /THYRIS/THYR(51), THYR2(51), DCCUR(10), DCK(10), DCT1(10),
3  1 DCT2(10), DCT3(10), DCK1(10), DCK2(10), DCMIN(10), DCMAX(10),
4  2 ACVA(10), ACVB(10), ACVC(10), PHSHIF(10),
5  3 ACVAI(10), ACVBI(10), ACVCI(10), COMR(10),
6  4 DCINI(10), DFREQ(10), ICON(51), IFIRE(51), NGROUP, IMODE(10),
7  5 NCOU(10)
8  DIMENSION DELAY(10), COUNT(51), EALFA(10), EMAX(10), CTIME(10),
9  1 EMIN(10), X(10), KPOS3(51), NMODE(10), CORDER(10),
10 2 CMARG(10), XCUR(10), XB(10)
11 DOUBLE PRECISION THYR, THYR2, DCCUR, DELTAT, DELAY, COUNT, DCK, DCK1,
12 1 DCK2, DCT1, DCT2, DCT3, DCMIN, DCMAX, DCINI, EALFA, DFREQ, EMAX, EMIN,
13 2 DELTA2, T, A, B, P, X, ACVA, ACVB, ACVC, PHSHIF, ACVAI, ACVBI, ACVCI,
14 3 CTIME, CORDER, CMARG, COMR, XCUR, XB
15 C ***** START CONTROL GROUP LOOP
16 DO 104 J=1, NGROUP
17 DCCUR(J)=DABS(DCCUR(J))
18 IF(ISTEP.GT.0) GO TO 101
19 C ***** INITIALIZATION BEFORE ENTERS TIME STEP LOOP
20 CORDER(J)=DCCUR(J)
21 CTIME(J)=0. DO
22 NMODE(J)=1
23 I=IMODE(J)
24 IF(IABS(I).GT.3)NMODE(J)=2
25 IF(I.LT.0)NMODE(J)=-NMODE(J)
26 IMODE(J)=IABS(I)-3*(IABS(NMODE(J))-1)
27 IF(J.GT.1) GO TO 103
28 DO 102 I=1, KSWTCH
29 COUNT(I)=0. DO
30 IFIRE(I)=0
31 102 CONTINUE
32 103 DELTA2=DELTAT/2. DO
33 DFREQ(J)=1. DO/(6.2831853DO*DFREQ(J))
34 T=DCT1(J)+DCT3(J)
35 P=DCT1(J)*DCT3(J)
36 A=1. DO+T/DELTA2+P/(DELTA2**2)
37 B=(1. DO+DCT2(J)/DELTA2)*DCK(J)
38 XB(J)=2. DO/B
39 DCT1(J)=4. DO*P/A/DELTAT
40 P=DCINI(J)
41 IF(IMODE(J).EQ.2)DCINI(J)=DCMAX(J)
42 IF(IMODE(J).EQ.3)DCINI(J)=DCMIN(J)
43 EMAX(J)=(DCMAX(J)-DCK1(J))/DCK2(J)
44 EMIN(J)=(DCMIN(J)-DCK1(J))/DCK2(J)
45 X(J)=0. DO
46 T=DCCUR(J)
47 IF(IMODE(J).GT.1)T=P
48 CMARG(J)=CORDER(J)-T
49 XCUR(J)=CORDER(J)-CMARG(J)-DCCUR(J)
50 EALFA(J)=(DCINI(J)-DCK1(J))/DCK2(J)
51 DCT2(J)=1. DO-DCK(J)*XB(J)
52 IF(IMODE(J).GT.1) XCUR(J)=EALFA(J)/DCK(J)
53 DCT3(J)=B/A
54 DCMAX(J)=2. DO*DCK(J)/A-DCT3(J)
55 DCK(J)=1. DO-2. DO/A
56 DCMIN(J)=DCMAX(J)*XCUR(J)+DCK(J)*EALFA(J)
57 GO TO 105
58 C ***** ON EACH TIME STEP
59 C ***** CALCULATE AMPLIFIER OUTPUT & DETERMINE OPERATING REGION
60 101 A=EALFA(J)

```

```

61      DCCUR(J)=CORDER(J)-DCCUR(J)-CMARG(J)
62      IF (IMODE(J).EQ.2.AND.DCCUR(J).GT.0.DO)GO TO 106
63      IF (IMODE(J).EQ.3.AND.DCCUR(J).LT.0.DO)GO TO 107
64      EALFA(J)=DCT3(J)*DCCUR(J)+DCMIN(J)
65      XCUR(J)=DCCUR(J)
66      X(J)=(EALFA(J)-A)/DELTA2-X(J)
67      IF (EALFA(J).GT.EMAX(J)) GO TO 106
68      IF (EALFA(J).LT.EMIN(J)) GO TO 107
69      IF (IMODE(J).GT.1)WRITE(6,300)J
70      300 FORMAT(' CONVERTER NO. ',I3,' BACK OFF FROM LIMIT')
71      IMODE(J)=1
72      GO TO 108
73      C ***** CONVERTER IN UPPER LIMIT
74      106 EALFA(J)=EMAX(J)
75      IF (IMODE(J).EQ.1)WRITE(6,301)J
76      301 FORMAT(' CONVERTER NO. ',I3,' HITS UPPER LIMIT')
77      XCUR(J)=EALFA(J)*XB(J)+DCT2(J)*XCUR(J)
78      IMODE(J)=2
79      X(J)=0.DO
80      GO TO 108
81      C ***** CONVERTER IN LOWER LIMIT
82      107 EALFA(J)=EMIN(J)
83      IF (IMODE(J).EQ.1)WRITE(6,302)J
84      302 FORMAT(' CONVERTER NO. ',I3,' HITS LOWER LIMIT')
85      XCUR(J)=EALFA(J)*XB(J)+DCT2(J)*XCUR(J)
86      IMODE(J)=3
87      X(J)=0.DO
88      108 DCMIN(J)=DCMAX(J)*XCUR(J)+DCK(J)*EALFA(J)+DCT1(J)*X(J)
89      105 IF (IABS(NMODE(J)).EQ.1.OR.1STEP.EQ.0)GO TO 160
90      A=6.2831853D0*DFREQ(J)
91      CTIME(J)=CTIME(J)+DELTAT
92      A=A-CTIME(J)
93      IF (A.GT.DELTA2) GO TO 104
94      CTIME(J)=0.DO
95      C ***** CALCULATING VALVE DELAY TIME
96      160 A=DCK1(J)+DCK2(J)*EALFA(J)
97      B=DABS(DCK1(J))
98      P=A/B
99      DELAY(J)=DFREQ(J)*DARCO5(P)
100     IF (NCDUT(J).EQ.0) GO TO 104
101     C ***** OUTPUT DELAY ON REQUEST
102     WRITE (6,11) J,DELAY(J)
103     11 FORMAT(1H,' CONVERTER NO. ',I3,2X,' DELAY IS',E15.6,' SEC. ')
104     CONTINUE
105     C ***** START VALVE COUNT LOOP
106     DO 100 I=1,KSWTCH
107     K=IABS(KPOS3(I))
108     IF (K.NE.4) GO TO 135
109     J=ICON(I)
110     IF (J.LE.0)GO TO 100
111     J=J/10
112     JJ=ICON(I)-J*10
113     IFIRE(I)=0
114     IF (PHSHIF(J).EQ.0.DO)GO TO 137
115     C ***** CALCULATE THE COMMUTATING VOLTAGES
116     C ***** CONVERTER TRANSFORMER WYE-DELTA CONNECTED
117     GO TO (141,142,143,144,145,146),JJ
118     141 A=-1.DO*ACVC(J)
119     GO TO 117
120     142 A=ACVB(J)

```

```

121      GO TO 117
122      143 A=-1.D0*ACVA(J)
123      GO TO 117
124      144 A=ACVC(J)
125      GO TO 117
126      145 A=-1.D0*ACVB(J)
127      GO TO 117
128      146 A=ACVA(J)
129      GO TO 117
130      C      ***** CONVERTER TRANSFORMER WYE-WYE CONNECTED
131      137 GO TO(111,112,113,114,115,116),JJ
132      111 A=ACVA(J)-ACVC(J)
133      GO TO 117
134      112 A=ACVB(J)-ACVC(J)
135      GO TO 117
136      113 A=ACVB(J)-ACVA(J)
137      GO TO 117
138      114 A=ACVC(J)-ACVA(J)
139      GO TO 117
140      115 A=ACVC(J)-ACVB(J)
141      GO TO 117
142      116 A=ACVA(J)-ACVB(J)
143      117 IF(NMODE(J).LT.0)A=-A
144      IF(ISTEP.GT.0)GO TO 118
145      IF(PHSHIF(J).EQ.0.D0)GO TO 138
146      GO TO (151,152,153,154,155,156),JJ
147      151 P=-1.D0*ACVCI(J)
148      GO TO 120
149      152 P=ACVBI(J)
150      GO TO 120
151      153 P=-1.D0*ACVAI(J)
152      GO TO 120
153      154 P=ACVCI(J)
154      GO TO 120
155      155 P=-1.D0*ACVBI(J)
156      GO TO 120
157      156 P=ACVAI(J)
158      GO TO 120
159      138 GO TO (121,122,123,124,125,126),JJ
160      121 P=ACVAI(J)-ACVCI(J)
161      GO TO 120
162      122 P=ACVBI(J)-ACVCI(J)
163      GO TO 120
164      123 P=ACVBI(J)-ACVAI(J)
165      GO TO 120
166      124 P=ACVCI(J)-ACVAI(J)
167      GO TO 120
168      125 P=ACVCI(J)-ACVBI(J)
169      GO TO 120
170      126 P=ACVAI(J)-ACVBI(J)
171      120 IF(NMODE(J).LT.0)P=-P
172      T=DATAN2(P,A)+1.570796327D0
173      IF(T.LT.0.D0)T=T+6.283185307D0
174      IF(NMODE(J).GT.0)GO TO 132
175      IF(T.GT.4.276056675D0)GO TO 100
176      GO TO 131
177      132 IF(T.GT.3.441592654D0)GO TO 100
178      131 COUNT(I)=T*DFREQ(J)
179      GO TO 119
180      C      ***** GENERATION OF FIRING PULSES

```

```
181      118 IF (A. LE. 0. DO) GO TO 133
182      COUNT(I)=COUNT(I)+DELTAT
183      119 T=DELAY(J)-COUNT(I)
184      IF (T. GE. DELTA2) GO TO 100
185      IFIRE(I)=1
186      133 COUNT(I)=0. DO
187      GO TO 100
188      135 IFIRE(I)=0
189      100 CONTINUE
190      RETURN
191      END
```

## APPENDIX 2

## Modifications in the Transients Program

To incorporate the converter model into the U.B.C. Electro-magnetic Transients Program, modifications have to be made in the program so that information may be transferred between the main program and the subroutine. The required changes are shown in the FORTRAN listings of Table A2-1.

## Explanation of Changes.

<u>File line no.</u>	<u>Comments</u>
53-59.2, 97.2-98	New variables for collecting information required by VALCON.
393-395, 450-451	Reset variables.
399-429, 571	Input control parameters.
1296.06-1296.9	Store node voltages for commutation voltage calculation before entering the time step loop.
1680.2-1681	Call subroutine VALCON.
1687-1687.2	Calculate group number.
1723, 1795	Store valve voltage and current.
1726-1728	Determine the ignition of valves.
1764.2, 1795.2	Avoid premature blocking after the valve fired which cause small current oscillation.
1796	Store dc line current.
1776.2	To make the switch open exactly at time $t=0$ .
1767, 1823	Reset valve voltage and current.
1820	Reset dc line current.
2053.05-2053.6	Store node voltages for commutation voltage calculation at each time step.

TABLE A2.1

Changes in the Transients Program for data transferred to subroutine VALCON

C=Change

I=Insertion

```

51      DIMENSION KMS(650),YS(650)
52      COMMON/HERMAN/          VOLT1(50),VOLTK(50),VOLT(50),VIM(50)
C 53      DIMENSION ADELAY(51),XMAX(50),XOUT(100),POLAR(51),JJJ(380)
53.2    C FOLLOWING DIMENSION STATEMENT PERTAINS TO VALVE CONTROL PARAMETERS
54      COMMON /THYRIS/THYR(51),THYR2(51),DCCUR(10),DCK(10),DCT1(10),
55      1 DCT2(10),DCT3(10),DCK1(10),DCK2(10),DCMIN(10),DCMAX(10),
56      2 ACVA(10),ACVB(10),ACVC(10),PHSHIF(10),
I 56.2    3 ACVAI(10),ACVBI(10),ACVCI(10),COMR(10),
57      4 DCINI(10),DFREQ(10),ICON(51),IFIRE(51),NGROUP,IMODE(10),
57.2    5 NCOUT(10)
58      DOUBLE PRECISION THYR,THYR2,DCCUR,DCK,DCT1,DCT2,DCT3,DCK1,DCK2,
59      1 DCMIN,DCMAX,DCINI,DFREQ,ACVA,ACVB,ACVC,PHSHIF,
59.2    2 ACVAI,ACVBI,ACVCI,COMR
60      DOUBLE PRECISION COPT,C,R,CK,CREST,BUS,XOPT,TR,TIME,TSTART,TCLOSE,

.....

96      C HISTORY OF DISTRIBUTED LINES IS CHANGED
97      LPAST=1250
I 97.2    C CHANGE FOLLOWING STATEMENT IF DIMENSION OF CONTROL GROUP IS CHANGED
98      LGROUP=10

.....

390      KSWTCH=0
391      KCONST=0
392      N4=0
I 393      NGROUP=0
394      DO 229 I=1,LBUS
395      229 JJJ(I)=0
396      209 KSWTCH=KSWTCH+1
397      READ(5,77)IT2
398      77  FORMAT(I2)
399      IF(IT2.NE.16)GO TO 199
400      IPRINT=16
401      IF(NGROUP.GT.LGROUP)GO TO 9000
402      NGROUP=NGROUP+1
403      KSWTCH=KSWTCH-1
404      BACKSPACE 5
405      READ(5,89) N2,IMODE(NGROUP),DCK(NGROUP),DCINI(NGROUP),
406      1 DCT1(NGROUP),DCT2(NGROUP),DCT3(NGROUP),DCCUR(NGROUP)
407      89  FORMAT(I2,6X,I2,6E10.6)
I 408      WRITE(6,179) N2,IMODE(NGROUP),DCK(NGROUP),DCINI(NGROUP),
409      1 DCT1(NGROUP),DCT2(NGROUP),DCT3(NGROUP),DCCUR(NGROUP)
410      179  FORMAT(' CONTROL PARAMETERS: '/1X,I2,10X,I4,6E14.6)
411      READ(5,159)DCK1(NGROUP),DCK2(NGROUP),DCMIN(NGROUP),DCMAX(NGROUP),
412      1 DFREQ(NGROUP),NCOUT(NGROUP)
413      159  FORMAT(10X,5E10.6,19X,I1)
414      WRITE(6,149)DCK1(NGROUP),DCK2(NGROUP),DCMIN(NGROUP),DCMAX(NGROUP)
415      1 DFREQ(NGROUP)
416      149  FORMAT(1H,16X,5E14.6)
417      READ(5,139)(VOLT(K),K=1,3),PHSHIF(NGROUP),COMR(NGROUP)
418      139  FORMAT(2X,3A6,2E10.6)
419      WRITE(6,129)(VOLT(K),K=1,3),PHSHIF(NGROUP),COMR(NGROUP)
I 420      129  FORMAT(10X,3(A6,2X),2E14.6)

```

TABLE A2.1 (cont'd)

```

421      DO 239 J=1,3
422      A=VOLT(J)
423      DO 249 I=2,NTOT
424      IF(A.EQ.BUS(I))GO TO 259
I 425      249 CONTINUE
425.6    WRITE(6,1042) A
425.65   GO TO 239
425.7    259 JJJ(I)=NGROUP*10+J
425.75   239 CONTINUE
426      GO TO 209
C 427      199 BACKSPACE 5
428      READ(5,35)IT2,BUS1,BUS2,BUS3,BUS4,CK1,A,JJ,J
429      35 FORMAT(12,2A6,4E10.6,23X,12,I1)

.....

448      212 ISOURC(KSWTCH)=0
449      ENERGY(KSWTCH)=0.0D0
I 450      THYR(KSWTCH)=0.0D0
451      THYR2(KSWTCH)=0.0D0
452      IF(J.LT.2) GO TO 224

.....

570      CRIT(KSWTCH)=CK1
I 571      ICON(KSWTCH)=JJ
572      GO TO 209
573      213 DO 214 I=2,NTOT

.....

1295      C
1296      590 L=1
1296.06   DO 3711 I=2,NTOT
1296.12   JJ=JJJ(I)
1296.18   IF(JJ.LE.0) GO TO 3711
1296.24   NJ=JJ/10
1296.3    JJ=JJ-NJ*10
1296.36   GO TO(3712,3713,3714),JJ
I 1296.42  3712 ACVA(NJ)=E(I)
1296.48   ACVAI(NJ)=F(I)
1296.54   GO TO 3711
1296.6    3713 ACVB(NJ)=E(I)
1296.66   ACVBI(NJ)=F(I)
1296.72   GO TO 3711
1296.78   3714 ACVC(NJ)=E(I)
1296.84   ACVCI(NJ)=F(I)
1296.9    3711 CONTINUE
1297      II=0

```

BEGIN OF LOOP FOR ADMITTANCE M



TABLE A2.1 (cont'd) -

BEGIN OF TIME-STEPS

```

1678      C
1679      1000 KCOUNT=NV
1680      IF(KSWTCH.EQ.0) GO TO 1009
I 1680.2  IF (NGROUP.LE.0) GO TO 3722
1681      CALL VALCON(ISTEP,DELTAT,KSWTCH,KPOS3)
1682      C
1683      3722 DO 1003 K=1,KSWTCH
1684          II=KPOS3(K)
1685          IT1=KPOS1(K)
1686          ICHECK=KPOS2(K)
I 1687      JJ=ICON(K)
1687.2  IF(JJ.GT.0)JJ=JJ/10
1688      I=IABS(II)

1721      2103 CK1=E(N2)-E(N1)
I 1722      A=(CK1+ENERGY(K))*0.5DO*POLAR(K)
1723      THYR2(K)=CK1*POLAR(K)
1724      ENERGY(K)=CK1
I 1726      IF(JJ.LE.0)GO TO 2122
1727      IF(IFIRE(K).LE.0)GO TO 1002
1727.2  IF(ISTEP.EQ.0) GO TO 2123
C 1727.4  2122 IF(A.LE.0.DO) GO TO 1002
1728      2123 I=3
1729      GO TO 2105

1763      2102 I=1
1764      2105 TCLOSE(K)=0.DO
I 1764.2  IF(I.EQ.3)ADELAY(K)=T+TOPEN(K)
1765      IF(TCL.GE.0.DO) TCL=T
1766      KONTRL=4
I 1767      THYR2(K)=0.DO
1768      WRITE(6,2107) TCL

1773      2108 IF(T.LT.TCL      ) GO TO 1002
1774      I=2
I 1775      IF(JJ.GT.0) GO TO 2105
1776      IF(II.GT.0 .AND. TOPEN(K).GT.TMAX) I=0
I 1776.2  IF(TCL.LT.0.DO.AND. TOPEN(K).LT.DELTA2)GO TO 2110
1777      GO TO 2105
1778      2110 L=N2

1794      IF(I.EQ.3) BUS1=-A*POLAR(K)
I 1795      THYR(K)=BUS1
1795.2  IF (I.EQ.3.AND. ADELAY(K).GT.T)BUS1=1.DO
1796      IF(I.EQ.2.AND. JJ.GT.0) DCCUR(JJ)=-A*POLAR(K)
1797      IF(ISSS.LE.0) GO TO 2112

```

TABLE A2.1 (cont'd)

```

1818      2118 TCLOSE(K)=0. DO
1819      IF(I. EQ. 3) I=5
I 1820      IF(I. EQ. 5. AND. JJ. GT. 0) DCCUR(JJ)=0. DO
1821      ENERGY(K)=0. DO
1822      KONTRL=3
I 1823      THYR(K)=0. DO
1824      WRITE(6, 2114) T

```

```

2052      1200 K=K+IT2
2053      IF(K. LE. 1BR) GO TO 1100
2053. 05    DO 1601 I=2, NTOT
2053. 1      JJ=JJJ(I)
2053. 15    IF(JJ. LE. 0) GO TO 1601
2053. 2      NJ=JJ/10
2053. 25    JJ=JJ-NJ*10
I 2053. 3      GO TO (1602, 1603, 1604), JJ
2053. 35    1602 ACVA(NJ)=E(I)
2053. 4      GO TO 1601
2053. 45    1603 ACVB(NJ)=E(I)
2053. 5      GO TO 1601
2053. 55    1604 ACVC(NJ)=E(I)
2053. 6      1601 CONTINUE
2054      IF(NV. EQ. 0) GO TO 1202

```

## APPENDIX 3

## Fourier Analysis Programme Listings

```

1  C FOURIER ANALYSIS PROGRAM FOR DISCRETE POINTS READ IN FROM DEVICE 4
2  DOUBLE PRECISION CTIME, GK2, X, TSTART, C1, GK1, S1, GK, AN, CP, AP, S,
3  1  BP, A, B, F, BUS, PAIR
4  DIMENSION A(1001), B(1001), F(5000), TEXT(17), Y(100), BUS(100),
5  1  PAIR(200)
6  1  READ(5, 2) CTIME, TSTART, IDPT, MLIM, INUMB
7  2  FORMAT(2F10. 5, I2, 2I3)
8  IF(INUMB. LT. 1) STOP
9  REWIND 4
10 READ(4) TEXT
11 READ(4) NT, DELTAT, IMAX, (BUS(I), I=1, NT)
12 READ(4) L, NV, NI, (PAIR(I), I=1, L)
13 NT=0
14 51 NT=NT+1
15 IF(NT. GT. 5000) GO TO 56
16 READ(4) K, KONTRL, ISTEP, (Y(I), I=1, K)
17 F(NT)=Y(INUMB)
18 IF(KONTRL. EQ. 1) GO TO 50
19 GO TO 51
20 50 NSTART=TSTART/DELTAT
21 IF((TSTART/DELTAT-NSTART). GT. 0. 5) NSTART=NSTART+1
22 N=CTIME/DELTAT
23 IF((CTIME/DELTAT-N). GT. 0. 5) N=N+1
24 NM=NSTART+N
25 BEGINT=NSTART*DELTAT
26 REALCY=N*DELTAT
27 K=1
28 NPLUS=NSTART+1
29 DO 52 I=NPLUS, NM
30 F(K)=F(I)
31 52 K=K+1
32 WRITE(6, 5) INUMB, (TEXT(I), I=1, 17), N, (F(K), K=1, N)
33 5 FORMAT(35H1FOURIER ANALYSIS FOR OUTPUT NUMBER , I5, ' OF ', 17A4, /23H
34 10RECORD OF ORDINATES IN, I4, 19H EQUIDISTANT POINTS / (1H , 6F18. 7))
35 WRITE(6, 6) REALCY, BEGINT
36 61 FORMAT(/, 'CYCLE TIME=', F15. 10, 'SECOND', ' ANALYSIS
37 1 STARTS AT ', F15. 10, 'SECOND')
38 AN=N
39 AN=AN/2. 0
40 J=AN+1. 6
41 M=AN+1. 0
42 IF(MLIM. LT. 1) GO TO 62
43 IF(MLIM. LT. M) IDPT=0
44 IF(MLIM. LT. M) M=MLIM
45 62 C1=DCOS(3. 141593/AN)
46 S1=DSIN(3. 141593/AN)
47 CP=1. 0
48 SP=0.
49 L=0
50 10 L=L+1
51 IF(L. GT. M) GO TO 100
52 GK2=0.
53 GK1=0.
54 K=N
55 20 GK=F(K)+CP*GK1*2. 0-GK2
56 GK2=GK1
57 GK1=GK
58 K=K-1
59 IF(K. GT. 1) GO TO 20
60 AP=(F(1)+GK1*CP-GK2)/AN

```

```

61      BP=SP*GK1/AN
62      IF(L.EQ.1) GO TO 30
63      IF(L.NE.J) GO TO 40
64      BP=0.
65      30 AP=AP/2.
66      40 A(L)=AP
67      B(L)=BP
68      AP=C1*CP-S1*SP
69      SP=C1*SP+S1*CP
70      CP=AP
71      GO TO 10
72      100 WRITE(6,101)
73      101 FORMAT(21HFOURIER COEFFICIENTS/78H HARMONIC      CDS-COEFF.      SI
74      1N-COEFF.      MAGNITUDE  MULTIPLE OF FUNDAMENTAL)
75      CP=1.0/DSQRT(A(2)**2+B(2)**2)
76      DO 110 K=1,M
77      L=K-1
78      AP=DSQRT(A(K)**2+B(K)**2)
79      BP=AP*CP
80      110 WRITE(6,111) L,A(K),B(K),AP,BP
81      111 FORMAT(1H ,15,2X,4F15.6)
82      IF(10PT.LE.0) GO TO 1
83      AN=N
84      AN=6.283185/AN
85      DO 210 K=1,N
86      AP=K-1
87      AP=AP*AN
88      X=AP
89      SP=A(1)
90      DO 200 L=2,M
91      SP=SP+A(L)*DCOS(X)+B(L)*DSIN(X)
92      200 X=X+AP
93      210 F(K)=SP
94      WRITE(6,211)(F(K),K=1,N)
95      211 FORMAT(47HCOORDINATES RECOMPUTED WITH FOURIER COEFFICIENTS/(1H ,
96      1 6F18.7))
97      GO TO 1
98      56 WRITE(6,57)
99      57 FORMAT('COMPUTED POINTS ARE MORE THAN 5000. INCREASE THE DIMENSION
100      1 OF VARIABLE F AS PER NEED')
101      STOP
102      END

```

## APPENDIX 4

Line Parameters and Converter Station Parameters  
of the Pacific HVDC Intertie

The Pacific HVDC Intertie, which was commissioned on May 21, 1970, was the first overhead HVDC transmission system installed in North America. Fig. A4.1 shows the main circuit of the intertie. The northern section, including the Celilo Converter Station, is owned and operated by the Bonneville Power Administration (BPA), while the southern section and the Sylmar Converter Station is partly owned but operated by the Los Angeles Department of Water and Power (LADWP).

The Intertie is a bipolar (earth return) system with DC rated voltage of  $\pm 400$  KV and transmission power capacity of 1440 MW. The dc transmission line is 847 miles long and its line data is shown in Table A4-1.

The rated direct voltage of the dc line is obtained by using six series connected, six-pulse, three phase bridge groups, each rated 133 KV, 1800A. The equipment layouts of the Celilo and Sylmar Converter Stations are basically the same. The bridge circuit and the filter arrangement at Celilo are shown in Fig. A4-2 and Fig. A4-3, respectively.

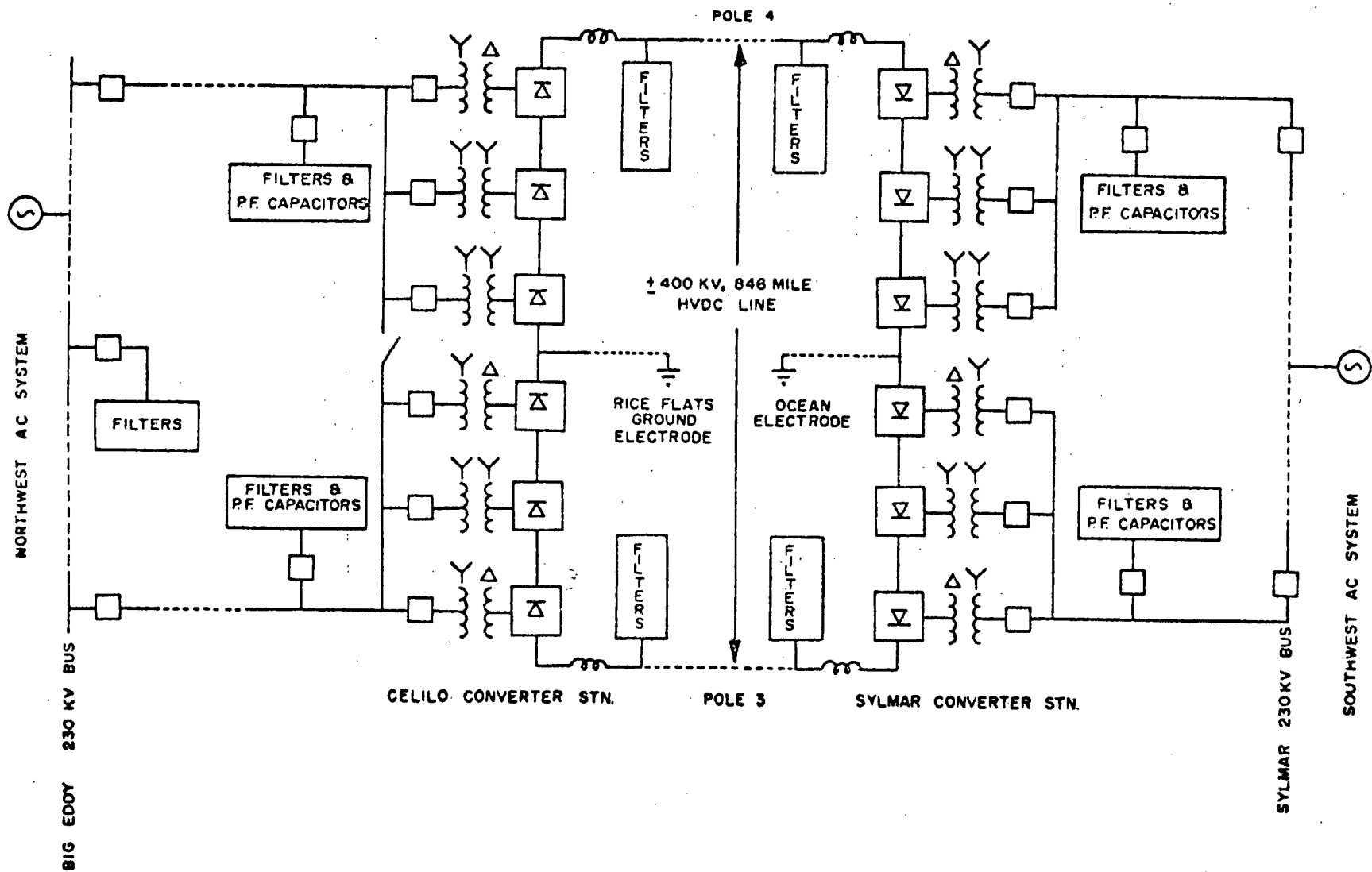


Fig. A4.1 MAIN CIRCUIT OF PACIFIC HVDC INTERTIE

PARAMETERS	MAIN LINE	GROUND WIRE
Number of subconductors	2	1
Subconductor diameter	4.577 cm	1.110 cm
Cross-sectional area of subconductor	1171 mm <sup>2</sup> (2312 MCM)	96.8 mm <sup>2</sup>
Bundle spacing	45.7 cm	
Nickname and composition of subconductor	Thrasher ACSR 76/19	ENS
Number of conductors	2 (pos. and neg.)	2
DC Resistance at 25°C	0.0125Ω/km/pole	
Total resistance at 1800 A	19.3Ω/pole	
Average max. height of conductors	24.84 m	33.83 m
Sag	11.55 m	11.55 m
Average height of conductors	18.45 m	26.13 m
Conductor spacing	12.19 m	5.49 m

TABLE A4.1 Transmission line data of the Pacific HVDC Intertie

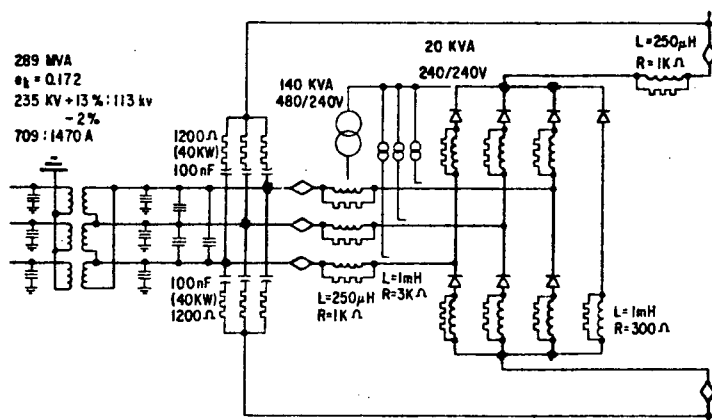


Fig. A4.2 Converter Bridge at Celilo

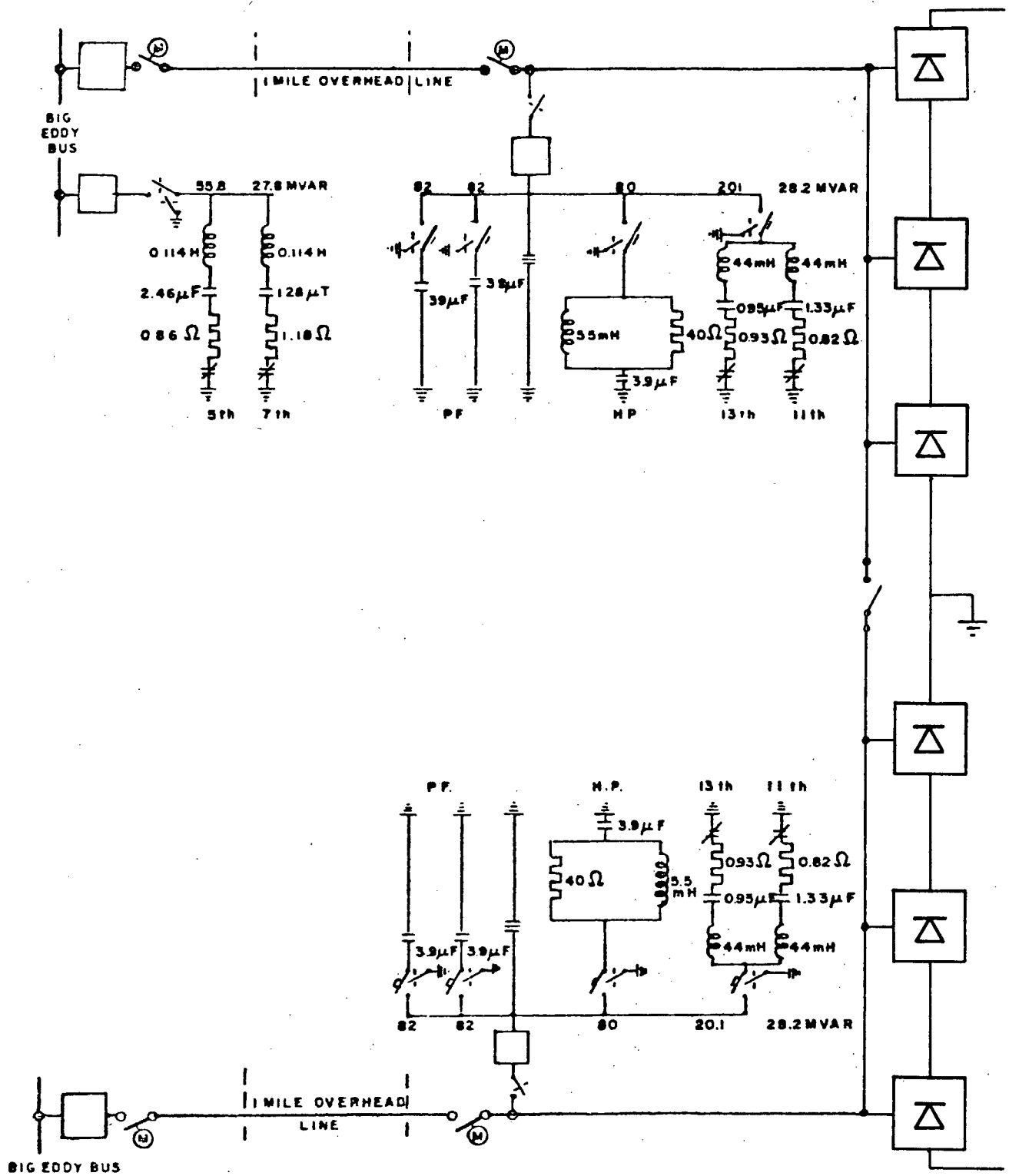


Fig. A4.3 FILTER ARRANGEMENT AT CELILO



## APPENDIX 5

## Input Listings of the Point to Point Operation Simulation

## (a) Simplified Model

```

1  CURRENT CONTROL SOURCE SIMULATION
2  50. E-6  75. E-3  2      1
3  VR      VRT      500.
4  VRT     CELEC     6.3    280.  7
5  VR      CELEC     900.0   .15
6  VR      CELEC     .001
7  VI      SELEC     .001
8  VI      SELEC     900.0   .15
9  VRT     CCAP      7
10 VRT     RF        2.5
11 RF      CELEC     7
12 RF      CELEC     100.
13 VIT     VI        500.
14 VIT     SELEC     6.3    280.  7
15 VIT     SCAP      7
16 VIT     IF        2.5
17 IF      SELEC     7
18 IF      SELEC     100.
19 CCAP
20 SCAP
21 CCAP     CELEC     .01
22 SCAP     SELEC     .01
23 CELEC
24 SELEC     .43    22.
25 CAN     CGR      1.
26 SAN     SGR      1.
27 CGR     CELEC     1.
28 SGR     SELEC     1.
29 CGR
30 SGR      .06
31 F        SW      5.00
32 -1VRT    F        .02    2.2   .0173 150.
33 -1F      VIT      .02    2.2   .0173 700.
34
35 SW      1. E-2  1.
36
37 16VR     1  1.39  133000.  4.4  0.04  0.0103  900.
38 16CAN    -148000. 14800.  -120000. 146000.
39 16SAN    3  1.39  800.0000  4.6  0.03  0.0125  900.
40 16VI     -148000. 14800.  -117700. -10000.
41
42 VRT     VR      VIT     VI
43
44
45
46

```

## (b) Detailed Model

1	PACIFIC HW-DC	INTERTIE	2
2	40. E-6	75. E-3	1 1 0 1
3	GENAS BICEA		.01
4	GENBS BICEB	GENAS BICEA	
5	GENCS BICEC	GENAS BICEA	
6	BICEA		.86 114. 2.46
7	BICEB	BICEA	
8	BICEC	BICEA	
9		BICEA	1.18 114. 1.28
10		BICEB	BICEA
11		BICEC	BICEA
12	BICEA CETA		.02 1.56
13	BICEB CETB	BICEA CETA	
14	BICEC CETC	BICEA CETA	
15	CETA CHPA		40.
16	CHPA CETA		5.5
17	CETB CHPB	CETA CHPA	
18	CHPB CETB	CHPA CETA	
19	CETC CHPC	CETA CHPA	
20	CHPC CETC	CHPA CETA	
21	CHPA		3.9
22	CHPB	CHPA	
23	CHPC	CHPA	
24		CETA	.93 44. .95
25		CETB	CETA
26		CETC	CETA
27	CETA C11A	GENAS BICEA	
28	CETB C11B	GENAS BICEA	
29	CETC C11C	GENAS BICEA	
30	C11A		.82 44. 1.33
31	C11B	C11A	
32	C11C	C11A	
33	C11A CTXAP		.22 2.07
34	C11B CTXBP	C11A CTXAP	
35	C11C CTXCP	C11A CTXAP	
36	51CTXAP		99300.
37	52CTXAS NS		47951. 23174.
38	1CTXBP	CTXAP	
39	2CTXDS NS		
40	1CTXCP	CTXAP	
41	2CTXCS NS		
42	NS		1. E+10
43	CTXAS CVDA		.07 .8343
44	CTXBS CVDB	CTXAS CVDA	
45	CTXCS CVDC	CTXAS CVDA	
46	CEL CVDA		1200. 0.0 .1
47	CEL CVDB	CEL CVDA	
48	CEL CVDC	CEL CVDA	
49	CAN CVDA	CEL CVDA	
50	CAN CVDB	CEL CVDA	
51	CAN CVDC	CEL CVDA	
52	CVDA CCA		1000.
53	CCA CVDA		.25
54	CVDB CCB	CVDA CCA	
55	CCB CVDB	CCA CVDA	
56	CVDC CCC	CVDA CCA	
57	CCC CVDC	CCA CVDA	
58	CIR1 CCTH		.01
59	CIR3 CCTH	CIR1 CCTH	
60	CIR5 CCTH	CIR1 CCTH	

61	CEL	CCTH	CVDA	CCA				
62	CCTH	CEL	CCA	CVDA				
63	CD1	CCA			3000.			
64	CCA	CD1				1.0		
64.2	CEL	CAN			1. E20			
64.4	SAN	SCTH			1. E20			
65	CD3	CCB	CD1	CCA				
66	CCB	CD3	CCA	CD1				
67	CD5	CCC	CD1	CCA				
68	CCC	CD5	CCA	CD1				
69	CD4	CAN	CD1	CCA				
70	CAN	CD4	CCA	CD1				
71	CD6	CAN	CD1	CCA				
72	CAN	CD6	CCA	CD1				
73	CD2	CAN	CD1	CCA				
74	CAN	CD2	CCA	CD1				
77	CAN	CGR				1.0		
78	CGR	CELEC	CAN	CGR				
79	CGR						.06	
80	1CELEC				.43	22.	.000	
81	CEL	POLES				500.0		
82	POLES	CELEC			6.3	280.	.7	
83	POLES	HPS					2.5	
84	HPS	CELEC			100.			
85	CELEC	HPS				7.0		
86	POLES	SURCS					.7	
87	SURCS						5.	
88	SURCS	CELEC	GENAS	BIGEA				
87	-1POLES	FAULT			.02	2.2	.0173	150.
90	-1FAULT	POLERR			.02	2.2	.0173	700.
91	SAN	SYL	CEL	POLES				
92	POLER	SELEC	POLES	CELEC				
93	POLER	HPR	POLES	HPS				
94	HPR	SELEC	HPS	CELEC				
95	SELEC	HPR	CELEC	HPS				
96	POLER	SURCR	POLES	SURCS				
97	SURCR		SURCS					
98	SURCR	SELEC	GENAS	BIGEA				
99	POLER	CAP	GENAS	BIGEA				
100	CAP						.06	
101	CAP	SYL				1.0		
102	STA	LA				1.0		
103	STB	LB	STA	LA				
104	STC	LC	STA	LA				
105	LA						.06	
106	LB		LA					
107	LC		LA					
108	LA	S57A	GENAS	BIGEA				
109	LB	S57B	GENAS	BIGEA				
110	LC	S57C	GENAS	BIGEA				
111	S57A				4.0	214.	1.32	
112	S57B		S57A					
113	S57C		S57A					
114		S57A			5.7	214.	.67	
115		S57B		S57A				
116		S57C		S57A				
117	S57A	S13A	GENAS	BIGEA				
118	S57B	S13B	GENAS	BIGEA				
119	S57C	S13C	GENAS	BIGEA				
120	S13A				1.8	44.	1.33	

121	S13B	S13A			
122	S13C	S13A			
123		S13A	2.2	44.	.95
124		S13B			
125		S13C			
126	S13A	SHPA	34.5		
126.2	SW		5.		
127	SHPA	S13A		4.8	
128	SHPA				4.5
128.1	CD1	CIR1			.001
128.11	CD3	CIR3	CD1	CIR1	
128.12	CD5	CIR5	CD1	CIR1	
128.13	CD4	CCA	CD1	CIR1	
128.14	CD6	CCB	CD1	CIR1	
128.15	CD2	CCC	CD1	CIR1	
129	S13B	SHPB	S13A	SHPA	
130	SHPB	S13B	SHPA	S13A	
131	SHPB		SHPA		
132	S13C	SHPC	S13A	SHPA	
133	SHPC	S13C	SHPA	S13A	
134	SHPC		SHPA		
135	S13A	GENAR	GENAS	BIGEA	
136	S13B	GENBR	GENAS	BIGEA	
137	S13C	GENCR	GENAS	BIGEA	
138	STA	STXAP	C11A	CTXAP	
139	STB	STXBP	C11A	CTXAP	
140	STC	STXCP	C11A	CTXAP	
141	1STXAP		CTXAP		
142	2STXAS	NR			
143	1STXBP		CTXAP		
144	2STXBS	NR			
145	1STXCP		CTXAP		
146	2STXCS	NR			
147	NR		NR		
148	STXAS	SVDA	CTXAS	CVDA	
149	STXBS	SVDB	CTXAS	CVDA	
150	STXCS	SVDC	CTXAS	CVDA	
151	SAN	SVDA	CEL	CVDA	
152	SAN	SVDB	CEL	CVDA	
153	SAN	SVDC	CEL	CVDA	
154	SCTH	SVDA	CEL	CVDA	
155	SCTH	SVDB	CEL	CVDA	
156	SCTH	SVDC	CEL	CVDA	
157	SIR2	SCTH	CIR1	CCTH	
158	SIR6	SCTH	CIR1	CCTH	
159	SIR4	SCTH	CIR1	CCTH	
160	SAN	SD1	CD1	CCA	
161	SD1	SAN	CCA	CD1	
162	SAN	SD3	CD1	CCA	
163	SD3	SAN	CCA	CD1	
164	SAN	SD5	CD1	CCA	
165	SD5	SAN	CCA	CD1	
166	SVDA	SD4	CD1	CCA	
167	SD4	SVDA	CCA	CD1	
168	SVDB	SD6	CD1	CCA	
169	SD6	SVDB	CCA	CD1	
170	SVDC	SD2	CD1	CCA	
171	SD2	SVDC	CCA	CD1	
171.03	CCA	CCAI1		.01	
171.06	CCB	CCB11		.01	

171.09	CCC	CCCII		01					
171.12	SVDA	SVDAII		01					
171.15	SVDB	SVDBII		01					
171.18	SVDC	SVDCII		01					
171.3	CCAI			87.22	112.94				
171.6	CCBI			87.22	112.94				
171.9	CCCI			87.22	112.94				
172.2	SVDAI			-73.24	125.14				
172.5	SVDBI			-73.24	125.14				
172.8	SVDCI			-73.24	125.14				
174	SCTH	SGR	CAN	CGR					
175		SELEC	CAN	CGR					
176	SGR		CGR						
177	1SELEC		CELEC						
178									
179	-1CIR1	CD1	0.0						
180	-1CIR3	CD3							
181	-1CIR5	CD5							
182	-1CCA	CD4							
183	-1CCB	CD6							
184	-1CCC	CD2	0.0						
186	-1SVDA	SD1							
187	-1SVDB	SD3	0.0						
188	-1SVDC	SD5	0.0						
189	-1SIR4	SD4	0.0						
190	-1SIR6	SD6							
191	-1SIR2	SD2							
191.02	CCAI	CCAI	-1.			1.E10			
191.04	CCBI	CCBI	-1.			1.E10			
191.06	CCCI	CCCI	-1.			1.E10			
191.08	SVDAI	SVDAI	-1.			1.E10			
191.1	SVDBI	SVDBI	-1.			1.E10			
191.12	SVDCI	SVDCI	-1.			1.E10			
191.2	16	4	1.39	133000.	4.4	0.04	.0103	900.	
191.23			-148000.	14800.	-120000.	146000.	60.		
191.26	C11A	C11B	C11C		7.18996				
191.29	16	-6	1.39	+735.00	4.6	0.03	.0125	900.	
191.32			-148000.	14800.	-117700.	-10000.	60.		
191.35	STA	STB.	STC		7.18996				
191.5	POLES	POLESS	-1.	1.5					
192	POLER	POLERR	-1.	1.5					
192.2	FAULT	SW	.01	1.5					
193									
194	14GENAS	191880.	60.		-60.			-1.	
195	14GENBS	191880.	60.		130.			-1.	
196	14GENCS	191880.	60.		+60.0			-1.	
197	14GENAR	177000.	60.		-60.			-1.	
198	14GENBR	177000.	60.		180.			-1.	
199	14GENCR	177000.	60.		+60.0			-1.	
200									
200.05	2CCTH	133000.							
200.1	2CEL	133000.							
200.15	2POLES	133000.							
200.2	2POLESS	133000.							
200.25	2FAULT	130300.							
200.3	2POLERR	117700.							
200.35	2POLER	117700.							
200.4	2CAP	117700.							
200.405	2SCTH	387.							
200.41	2SGR	387.							

200.415	2SELEC	387.	
200.42	2CELEC	-387.	
200.425	2CGR	-387.	
200.43	2CAN	-387.	
200.45	2SYL	117700.	
200.5	2SAN	140350.	
200.52	3SAN	SVDA	
200.525	3SAN	SVDB	140350.
200.53	3SAN	SVDC	
200.55	3CEL	POLES 900.	
200.6	3POLESS	FAULT 900.	
200.65	3FAULT	POLEERR900.	-900.
200.7	3POLER	CAP 900.	-900.
200.71	3CAP	SYL 900.	
200.72	3CAP		117700.
200.73	3CELEC	HPS	
200.74	3SELEC	HPR	
200.75	3POLES	SURCS	133000.
200.76	3POLER	SURCR	117700.
200.77	3POLES	HPS	133000.
200.78	3POLER	HPR	117700.
200.79	3POLES	CELEC	133000.
200.791	3CELEC		-900.
200.792	3SELEC		900.
200.793	3CAN	CGR	-900.
200.794	3CGR	CELEC	-900.
200.795	3CGR		
200.796	3SCTH	SGR 900.	
200.797	3SGR	SELEC 900.	
200.798	3SGR		
200.8	3POLER	SELEC	117700.
200.81	3SAN	SYL	-900.
200.82	3CCTH	CEL 900.	
201	CEL	SAN	
202			
203			

## APPENDIX 6

## Sample Data Deck of the Three-Terminal Operation Simulation

1	PACIFIC HV-DC INTERTIE				0
2	60. E-6	98. BE-3 -1	1	0	1
3	GENAS	BIGEA		.01	
4	GENBS	BIGEB	GENAS	BIGEA	
5	GENCS	BIGEC	GENAS	BIGEA	
6	BIGEA			.86	114. 2.46
7	BIGEB	BIGEA			
8	BIGEC	BIGEA			
9		BIGEA		1.18	114. 1.28
10		BIGEB	BIGEA		
11		BIGEC	BIGEA		
12	BIGEA	CETA		.02	1.56
13	BIGEB	CETB	BIGEA	CETA	
14	BIGEC	CETC	BIGEA	CETA	
15	CETA	CHPA		40.	
16	CHPA	CETA			5.5
17	CETB	CHPB	CETA	CHPA	
18	CHPB	CETB	CHPA	CETA	
19	CETC	CHPC	CETA	CHPA	
20	CHPC	CETC	CHPA	CETA	
21	CHPA				3.9
22	CHPB	CHPA			
23	CHPC	CHPA			
24		CETA		.93	44. .95
25		CETB	CETA		
26		CETC	CETA		
27	CETA	C11A	GENAS	BIGEA	
28	CETB	C11B	GENAS	BIGEA	
29	CETC	C11C	GENAS	BIGEA	
30	C11A			.82	44. 1.33
31	C11B	C11A			
32	C11C	C11A			
33	C11A	CTXAP		.22	2.07
34	C11B	CTXBP	C11A	CTXAP	
35	C11C	CTXCP	C11A	CTXAP	
36	51CTXAP			99300.	
37	52CTXAS	NS		47951.	23174.
38	1CTXBP	CTXAP			
39	2CTXBS	NS			
40	1CTXCP	CTXAP			
41	2CTXCS	NS			
43	CTXAS	CVDA		.07	.8343
44	CTXBS	CVDB	CTXAS	CVDA	
45	CTXCS	CVDC	CTXAS	CVDA	
46	CEL	CVDA		1200.	0.0 .1
47	CEL	CVDB	CEL	CVDA	
48	CEL	CVDC	CEL	CVDA	
49	CAN	CVDA	CEL	CVDA	
50	CAN	CVDB	CEL	CVDA	
51	CAN	CVDC	CEL	CVDA	
52	CVDA	CCA		1000.	
53	CCA	CVDA			.25
54	CVDB	CCB	CVDA	CCA	
55	CCB	CVDB	CCA	CVDA	
56	CVDC	CCC	CVDA	CCA	
57	CCC	CVDC	CCA	CVDA	
58	CIR1	CCTH		.01	
59	CIR3	CCTH	CIR1	CCTH	
60	CIR5	CCTH	CIR1	CCTH	
61	CEL	CCTH	CVDA	CCA	

62	CCTH	CEL	CCA	CVDA				
63	CD1	CCA			3000.			
64	CCA	CD1				1.0		
67	CD3	CCB	CD1	CCA				
68	CCB	CD3	CCA	CD1				
69	CD5	CCC	CD1	CCA				
70	CCC	CD5	CCA	CD1				
71	CD4	CAN	CD1	CCA				
72	CAN	CD4	CCA	CD1				
73	CD6	CAN	CD1	CCA				
74	CAN	CD6	CCA	CD1				
75	CD2	CAN	CD1	CCA				
76	CAN	CD2	CCA	CD1				
77	CAN	CGR				1.0		
78	CGR	CELEC	CAN	CGR				
79	CGR						.06	
80	1CELEC				.43	22.		
81	CEL	POLES				500.0		
81.2	SW11	POLERR				.015		
81.4	SW11	SW11I	GENAS	BIGEA				
81.5	SW12	SW12I	GENAS	BIGEA				
82	POLES	CELEC			6.3	280.	.7	
83	POLES	HPS					2.5	
84	HPS	CELEC			100.			
85	CELEC	HPS				7.0		
86	POLES	SURCS					.7	
87	SURCS						5.	
88	SURCS	CELEC	GENAS	BIGEA				
89	-1POLESSFAULT3				.015	4.27	.0142	600.
89.2	-2POLE4 FAULT4				.02	1.56	.0192	600.
90	-1FAULT3POLERR				.015	4.27	.0142	250.
90.2	-2FAULT4SW12				.02	1.56	.0192	250.
91	SAN	SYL	CEL	POLES				
92	POLR	SELEC	POLES	CELEC				
92.02	GENAS	BIGEA	GENAS	BIGEA				
92.04	GENDS	BIGEA	GENAS	BIGEA				
92.06	GENCS	BIGEA	GENAS	BIGEA				
92.08	BIGEA		BIGEA					
92.1	BIGEA		BIGEA					
92.12	BIGEA		BIGEA					
92.122		BIGEA		BIGEA				
92.124		BIGEA		BIGEA				
92.126		BIGEA		BIGEA				
92.14	BIGEA	CETAA	BIGEA	CETA				
92.16	BIGEA	CETBA	BIGEA	CETA				
92.18	BIGEA	CETCA	BIGEA	CETA				
92.2	CETAA	CHPAA	CETA	CHPA				
92.22	CETBA	CHPBA	CETA	CHPA				
92.24	CETCA	CHPCA	CETA	CHPA				
92.26	CHPAA	CETAA	CHPA	CETA				
92.28	CHPBA	CETBA	CHPA	CETA				
92.3	CHPCA	CETCA	CHPA	CETA				
92.32	CHPAA		CHPA					
92.34	CHPBA		CHPA					
92.36	CHPCA		CHPA					
92.38		CETAA		CETA				
92.4		CETBA		CETA				
92.42		CETCA		CETA				
92.44	CETAA	C11AA	CETA	C11A				
92.46	CETBA	C11BA	CETA	C11A				



92.48	CETCA	C11CA	CETA	C11A
92.5	C11AA		C11A	
92.52	C11BA		C11A	
92.54	C11CA		C11A	
92.56	C11AA	CTXPA	C11A	CTXAP
92.58	C11BA	CTXPB	C11A	CTXAP
92.6	C11CA	CTXPC	C11A	CTXAP
92.62	1CTXPA		CTXAP	
92.64	2CTXSA	ANS		
92.66	1CTXPB		CTXAP	
92.68	2CTXSB	ANS		
92.7	1CTXPC		CTXAP	
92.72	2CTXSC	ANS		
93	POLER	HPR	POLES	HPS
93.1	ACTH	AGR	CAN	CGR
93.15	AGR		CGR	
93.2	AGR	CELEC	CAN	CGR
93.3	AAN	ACEL	GENAS	BIGEA
93.35	ACEL	POLA	CEL	POLES
93.4	POLA	CELEC	POLES	CELEC
93.45	POLA	AHPS	POLES	HPS
93.5	AHPS	CELEC	HPS	CELEC
93.55	CELEC	AHPS	CELEC	HPS
93.6	POLA	ASUR	POLES	SURCS
93.65	ASUR		SURCS	
93.7	ASUR	CELEC	GENAS	BIGEA
94	HPR	SELEC	HPS	CELEC
95	SELEC	HPR	CELEC	HPS
96	POLER	SURCR	POLES	SURCS
97	SURCR		SURCS	
98	SURCR	SELEC	GENAS	BIGEA
99	POLER	CAP	GENAS	BIGEA
100	CAP			
100.2	CTXSA	AVDA	CTXAS	CVDA
100.4	CTXSB	AVDB	CTXAS	CVDA
100.6	CTXSC	AVDC	CTXAS	CVDA
101	CAP	SYL		
101.05	AAN	AVDA	CEL	CVDA
101.1	AAN	AVDB	CEL	CVDA
101.15	AAN	AVDC	CEL	CVDA
101.2	ACTH	AVDA	CEL	CVDA
101.25	ACTH	AVDB	CEL	CVDA
101.3	ACTH	AVDC	CEL	CVDA
101.35	AVDA	ACCA	CVDA	CCA
101.4	AVDB	ACCB	CVDA	CCA
101.45	AVDC	ACCC	CVDA	CCA
101.5	ACCA	AVDA	CCA	CVDA
101.55	ACCB	AVDB	CCA	CVDA
101.6	ACCC	AVDC	CCA	CVDA
101.65	ACIR4	ACTH	CIR1	CCTH
101.67	ACIR6	ACTH	CIR1	CCTH
101.69	ACIR2	ACTH	CIR1	CCTH
101.71	AAN	ACD1	CD1	CCA
101.73	AAN	ACD3	CD1	CCA
101.75	AAN	ACD5	CD1	CCA
101.77	ACCA	ACD4	CD1	CCA
101.79	ACCB	ACD6	CD1	CCA
101.81	ACCC	ACD2	CD1	CCA
101.83	ACD1	AAN	CCA	CD1
101.85	ACD3	AAN	CCA	CD1

101. 87	ACD5	AAN	CCA	CD1			
101. 89	ACD4	ACCA	CCA	CD1			
101. 91	ACD6	ACCB	CCA	CD1			
101. 93	ACD2	ACCC	CCA	CD1			
102	STA	LA			1. 0		
103	STB	LB	STA	LA			
104	STC	LC	STA	LA			
105	LA					. 06	
106	LB		LA				
107	LC		LA				
108	LA	S57A	GENAS	BIGEA			
109	LB	S57B	GENAS	BIGEA			
110	LC	S57C	GENAS	BIGEA			
111	S57A				4. 0	214.	1. 32
112	S57B		S57A				
113	S57C		S57A				
114		S57A			5. 7	214.	. 67
115		S57B		S57A			
116		S57C		S57A			
117	S57A	S13A	GENAS	BIGEA			
118	S57B	S13B	GENAS	BIGEA			
119	S57C	S13C	GENAS	BIGEA			
120	S13A				1. 8	44.	1. 33
121	S13B		S13A				
122	S13C		S13A				
123		S13A			2. 2	44.	. 95
124		S13B		S13A			
125		S13C		S13A			
126	S13A	SHPA			34. 5		
127	SW				5.		
128	SHPA	S13A				4. 8	
129	SHPA						4. 5
136	S13B	SHPB	S13A	SHPA			
137	SHPB	S13B	SHPA	S13A			
138	SHPB		SHPA				
139	S13C	SHPC	S13A	SHPA			
140	SHPC	S13C	SHPA	S13A			
141	SHPC		SHPA				
142	S13A	GENAR	GENAS	BIGEA			
143	S13B	GENBR	GENAS	BIGEA			
144	S13C	GENCR	GENAS	BIGEA			
145	STA	STXAP	C11A	CTXAP			
146	STB	STXBP	C11A	CTXAP			
147	STC	STXCP	C11A	CTXAP			
148	1STXAP		CTXAP				
149	2STXAS	NR					
150	1STXBP		CTXAP				
151	2STXBS	NR					
152	1STXCP		CTXAP				
153	2STXCS	NR					
155	STXAS	SVDA	CTXAS	CVDA			
156	STXBS	SVDB	CTXAS	CVDA			
157	STXCS	SVDC	CTXAS	CVDA			
158	SAN	SVDA	CEL	CVDA			
159	SAN	SVDB	CEL	CVDA			
160	SAN	SVDC	CEL	CVDA			
161	SCTH	SVDA	CEL	CVDA			
162	SCTH	SVDB	CEL	CVDA			
163	SCTH	SVDC	CEL	CVDA			
164	SIR2	SCTH	CIR1	CCTH			

165	SIR6	SCTH	CIR1	CCTH	
166	SIR4	SCTH	CIR1	CCTH	
167	SAN	SD1	CD1	CCA	
168	SD1	SAN	CCA	CD1	
169	SAN	SD3	CD1	CCA	
170	SD3	SAN	CCA	CD1	
171	SAN	SD5	CD1	CCA	
172	SD5	SAN	CCA	CD1	
173	SVDA	SD4	CD1	CCA	
174	SD4	SVDA	CCA	CD1	
175	SVDB	SD6	CD1	CCA	
176	SD6	SVDB	CCA	CD1	
177	SVDC	SD2	CD1	CCA	
178	SD2	SVDC	CCA	CD1	
191	SCTH	SGR	CAN	CGR	
192	SGR	SELEC	CAN	CGR	
193	SGR		CGR		
194	1SELEC		CELEC		
194.05	CCAI			59.93	296.
194.1	CCBI			59.93	296.
194.15	CCCI			59.93	296.
194.2	SVDAI			-90.7	627.
194.25	SVDBI			-90.7	627.
194.3	SVDCI			-90.7	627.
194.35	ACCAI			-99.3	618.
194.4	ACCB			-99.3	618.
194.45	ACCCI			-99.3	618.
194.5	CCA	CCAI	GENAS	BIGEA	
194.55	CCB	CCBI	GENAS	BIGEA	
194.6	CCC	CCCI	GENAS	BIGEA	
194.65	ACCA	ACCAI	GENAS	BIGEA	
194.7	ACCB	ACCB	GENAS	BIGEA	
194.75	ACCC	ACCCI	GENAS	BIGEA	
194.8	SVDA	SVDAI	GENAS	BIGEA	
194.85	SVDB	SVDBI	GENAS	BIGEA	
194.9	SVDC	SVDCI	GENAS	BIGEA	
195					
196	-1CIR1	CD1	0.0		
197	-1CIR3	CD3			
198	-1CIR5	CD5			
199	-1CCA	CD4			
200	-1CCB	CD6			
201	-1CCC	CD2	0.0		
202	-1SVDA	SD1			
203	-1SVDB	SD3	0.0		
204	-1SVDC	SD5	0.0		
205	-1SIR4	SD4	0.0		
206	-1SIR6	SD6			
207	-1SIR2	SD2			
207.005	CCAI	CCAI	-1.	1.E10	
207.01	CCBI	CCBI	-1.	1.E10	
207.015	CCCI	CCCI	-1.	1.E10	
207.02	SVDAI	SVDAI	-1.	1.E10	
207.025	SVDBI	SVDBI	-1.	1.E10	
207.03	SVDCI	SVDCI	-1.	1.E10	
207.035	ACCAI	ACCAI	-1.	1.E10	
207.04	ACCB	ACCB	-1.	1.E10	
207.045	ACCCI	ACCCI	-1.	1.E10	
207.1	-1ACCA	ACD1			
207.2	-1ACCB	ACD3			

207.3	-1ACCC	ACD5					
207.4	-1ACIR4	ACD4					
207.5	-1ACIR6	ACD6					
207.6	-1ACIR2	ACD2					
214	16	2	1.39	800.000	4.6	0.03	.0125 700.
215			-148000.	14800.	-70000.0	-79000.0	60.
216	C11A	C11B	C11C		7.18996		
217	16	-1	1.39	-58000.	4.4	0.04	.0103 370.
218			-158000.	14800.	-80000.0	-10000.	60.
219	STA	STB	STC		7.18996		
219.2	16	-1	1.39	-52500.	4.6	0.03	.0125 370.
219.4			-162000.	15300.	-120000.	-10000.	60.
219.6	C11AA	C11BA	C11CA		7.18996		
220	POLES	POLESS	-1.	1.5			
221	POLER	POLERR	-1.	1.5			
221.2	POLE4	POLA	-1.	1.5			
221.4	SW11I	SW12I	-1	1.5			
222	SW12	SW	.01	1.5			
223							
224	14GENAS	187770.	60.		-50.		-1.
225	14GENBS	187770.	60.		-170.		-1.
226	14GENCS	187770.	60.		+70.0		-1.
227	14GENAR	177000.	60.		-50.		-1.
228	14GENRR	177000.	60.		-170.		-1.
229	14GENCR	177000.	60.		+70.0		-1.
230							
231	2CCTH	70000.					
232	2CEL	70000.					
233	2POLES	70000.					
234	2POLESS	70000.					
235	2FAULT3	62370.					
235.05	2FAULT4	56400.					
235.1	2POLE4	52500.					
235.15	2POLA	52500.					
235.2	2ACEL	52500.					
235.25	2SW11	58000.					
235.255	2SW12I	58000.					
235.27	2SW11I	58000.					
235.3	2SW12	58000.					
235.35	2AAN	52500.					
235.4	2ACTH	-132.					
235.45	2AGR	-132.					
236	2POLERR	58000.					
237	2POLER	58000.					
238	2CAP	58000.					
239	2SCTH	132.					
240	2SOR	132.					
241	2SELEC	132.					
242	2CELEC	-132.					
243	2CCR	-132.					
244	2CAN	-132.					
245	2SYL	58000.					
246	2SAN	140350.					
247	3SAN	SVDA					
248	3SAN	SVDB					
249	3SAN	SVDC					
250	3CEL	POLES 640.					
251	3POLESS	FAULT3640.			-640.		
251.2	3POLE4	FAULT4-370.			370.		
252	3FAULT3	POLERR640.			-640.		

252. 2	3FAULT4SW12	-370.	370.
253	3POLER CAP	370.	
254	3CAP SYL	370.	
255	3CAP		58000.
256	3CELEC HPS		
257	3SELEC HPR		
258	3POLES SURCS		70000.
258. 1	3POLA ASUR		52500.
258. 2	3POLA AHPS		52500.
258. 3	3POLA CELEC		52500.
258. 4	3CELEC AHPS		
259	3POLER SURCR		58000.
260	3POLES HPS		70000.
261	3POLER HPR		58000.
262	3POLES CELEC		70000.
263	3CELEC	-370.	
264	3SELEC	370.	
265	3CAN CGR	-640.	
266	3CGR CELEC	-640.	
266. 1	3ACEL POLA	-370.	
266. 2	3ACTH AGR	370.	
266. 3	3AGR CELEC	370.	
266. 4	3AGR		
267	3CGR		
268	3SCTH SGR	370.	
269	3SGR SELEC	370.	
270	3SGR		
271	3POLER SELEC		58000.
271. 1	3SW11 POLERR	-370.	
271. 2	3SURCS		
271. 3	3SURCR		
271. 4	3ASUR		
272	3SAN SYL	-370.	
273	3CCTH CEL	640.	
274	SW11 POLE4 POLES		
275			
276			